ANL-HEP-PR-95-12

arXiv:hep-ph/9503294v2 12 Mar 1995

# PROPERTIES OF THE SCALE INVARIANT $O(g^4)$ LIPATOV KERNEL

Claudio Corianò and Alan R. White *
High Energy Physics Division,
Argonne National Laboratory,
Argonne, IL 60439.

**Abstract**

We study the scale-invariant $O(g^4)$ kernel which appears as an infra-red contribution in the BFKL evolution equation and is constructed via multiparticle $t$-channel unitarity. We detail the variety of Ward identity constraints and infra-red cancellations that characterize its infrared behaviour. We give an analytic form for the full non-forward kernel. For the forward kernel controlling parton evolution at small-x, we give an impact parameter representation, derive the eigenvalue spectrum, and demonstrate a holomorphic factorisation property related to conformal invariance. The results show that, at next-to-leading-order, the transverse momentum infra-red region may produce a strong reduction of the BFKL small-x behavior.

*Work supported by the U.S. Department of Energy, Division of High Energy Physics, Contract W-31-109-ENG-38

# 1. INTRODUCTION

The BFKL equation[1] describes the leading log small-x evolution of parton distributions in QCD. In recent papers[2, 3] we have proposed that a scale-invariant approximation to the next-to-leading order kernel can be directly constructed from $t$-channel unitarity. We have also presented[4] results on the structure and eigenvalue spectrum of the new, $O(g^4)$, kernel. Our purpose in this paper is to derive various properties of this kernel which have been utilised in [4], to elaborate on derivations outlined there, and also to describe additional new results.

In a companion paper[5] we give a full discussion of the $t$-channel unitarity derivation of reggeon kernels which was only sketched in [3]. We show how the angular momentum plane structure of a gauge theory can be obtained by expanding around $j = 1$ (the analogue of expanding in powers of logarithms in momentum space) in combination with the Ward identity constraints and group structure that define the theory. At $O(g^4)$, the four-particle nonsense states provide an unambiguous infra-red contribution which can be written as the sum of scale-invariant transverse momentum integrals that we study in this paper. Here we will not discuss either this derivation or the very important issue of how the relevant physical scales should be introduced. Although this is crucial for determining physical contributions correctly, we believe the mathematical properties of the new kernel are of sufficient interest in their own right.

We will particularly emphasize those properties that the new kernel shares with the $O(g^2)$ kernel. It is, of course, scale-invariant, it is also infra-red finite, both before integration and as an integral kernel, and satifies Ward Identity constraints at zero momentum transfer. In addition we will show that there is a component of the parton evolution kernel (that is the forward kernel) which is separately infra-red finite and whose eigenvalue spectrum shares many properties of the spectrum of the $O(g^2)$ kernel. In particular we are able demonstrate the important property of holomorphic factorization for the eigenvalues which is closely related to conformal symmetry in the conjugate impact parameter space[6].

We begin by reviewing the BFKL kernel in Section 2. This serves to introduce language and to focus on those properties of the leading-order kernel which we generalize. In Section 3 we present the $O(g^4)$ kernel and elaborate on the variety of Ward identity properties and infra-red cancellations. Section 4 is devoted to the

evaluation of the two-dimensional box diagram as a sum of logarithms. This allows us to give an analytic expression for the complete kernel. The remaining Sections are devoted to the forward kernel. In Section 5 we discuss the structure of this kernel and also introduce a dimensionally regularized form to prepare for the eigenvalue evaluation. Section 6 contains expressions in impact parameter space for the distinct components of the forward kernel. In Section 7 we compute the spectrum of both the four-particle kernel and the kernel introduced in [4] which contains also two-particle nonsense states. We show that a large reduction of the BFKL power growth of parton distributions at small-x can occur. Finally we briefly discuss the significance of our results in a concluding Section.

## 2. THE $O(g^2)$ PARTON AND REGGEON KERNELS

In this Section we review properties of the BFKL equation and kernel[1, 7]. This will introduce our notation and establish various properties which we want to compare with for the $O(g^4)$ kernel.

The most familiar application of the BFKL equation is as an evolution equation for parton distributions at small-x i.e.

$$\frac{\partial}{\partial(ln1/x)}F(x,k^2) \;=\; \tilde{F}(x,k^2) \;+\; \frac{1}{(2\pi)^3}\int\frac{d^2k'}{(k')^4}\;K(k,k')F(x,k'^2) \tag{2.1}$$

where, if the gauge group is SU(N), the "parton" kernel $K(k,k')$ is given by

$$(Ng^2)^{-1}K(k,q) \;=\; \left(-\;\delta^2(k-k')k^6\int\frac{d^2p}{p^2(k-p)^2}\;+\;\frac{2k^2k'^2}{(k-k')^2}\right) \tag{2.2}$$

This equation originates, however, in Regge limit calculations[1] where also a non-forward (i.e.$q\neq 0$ in the following) version is derived. If we transform to $\omega$ - space (where $\omega$ is conjugate to $ln\,\frac{1}{x}$), we can write the full non-forward equation in the form

$$\omega F(\omega,k,q-k) \;=\; \tilde{F} \;+\; \frac{1}{16\pi^3}\int\frac{d^2k'}{(k')^2(k'-q)^2}\;K(k,k',q)F(\omega,k',q-k') \tag{2.3}$$

where the "reggeon" kernel $K(k,k',q) \;=\; K^{(2)}_{2,2}(q-k,k,k',q-k')$ now contains three kinematic forms. (Throughout this paper we normalise our transverse momentum

integrals by $(16\pi^3)^{-1}$, rather than $(2\pi)^{-3}$ as in our previous papers.) We write, therefore,

$$\begin{aligned}\frac{1}{Ng^2}\, K^{(2)}_{2,2}(k_1,k_2,k_3,k_4) \;&=\; \sum\Bigg( -\frac{1}{2}k_1^4 J_1(k_1^2)k_2^2(16\pi^3)\delta^2(k_2-k_3) \\ &\qquad + \frac{k_1^2k_3^2}{(k_1-k_4)^2} \;-\; \frac{1}{2}(k_1+k_2)^2\Bigg) \\ &\equiv\; K_1^{(2)} \;+\; K_2^{(2)} \;+ K_3^{(2)} \;\;.\end{aligned} \tag{2.4}$$

where

$$J_1(k^2) \;=\; \frac{1}{16\pi^3}\int \frac{d^2k'}{(k')^2(k'-k)^2} \tag{2.5}$$

and the $\sum$ implies that we sum over permutations of both the initial and the final state. That is, we add to the explicit expressions we have given, the same expressions with the suffices 1 and 2 interchanged and then add further expressions with 3 and 4 interchanged. (In previous papers we have used a notation involving summation over permutation of 1 and 2 only. The present notation is consistent with the diagrammatic notation we use.)

In the following we will utilise transverse momentum diagrams extensively. We construct these diagrams using the components illustrated in Fig. 2.1.

Fig. 2.1 (a)vertices and (b) intermediate states forming transverse momentum diagrams

For each vertex, illustrated in Fig. 2.1(a), we write a factor

$$16\pi^3\delta^2(\sum k_i \;-\sum k_i')(\sum k_i\;)^2$$

For each intermediate state, illustrated in Fig. 2.1(b), we write a factor

$$(16\pi^3)^{-n}\int d^2k_1...d^2k_n \;/\; k_1^2...k_n^2$$

We will define dimensionless kernels and components of kernels by including a factor $16\pi^3\delta^2(\sum k_i - \sum k'_i)$ in their definition. We denote this by a hat e.g.

$$\hat{K}^{(2)}_{2,2}(k_1,k_2,k_3,k_4) \;=\; 16\pi^3\delta^2(k_1+k_2-k_3-k_4)K^{(2)}_{2,2}(k_1,k_2,k_3,k_4)$$

(In [4] we did not use the hat but instead used a tilde to denote a kernel without the $\delta$-function.) This defines kernels that are formally scale-invariant (even though potentially infra-red divergent). The diagrammatic representation of $\hat{K}^{(2)}_{2,2}$ is then as shown in Fig. 2.2,

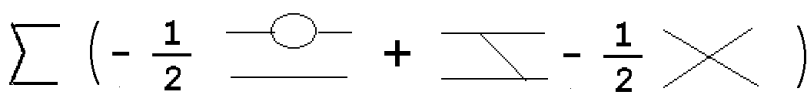

Fig. 2.2 Diagrammatic representation of $\hat{K}^{(2)}_{2,2}$

where the summation sign again implies a sum over all permutations of the initial and final momenta.

There are two crucial properties of $K^{(2)}_{2,2}$ that we will generalise in the following which are direct consequences of the gauge invariance of the theory.

- Ward identity constraints[2, 5] are satisfied i.e.

$$K^{(2)}_{2,2}(k_1,k_2,k_3,k_4) \;\rightarrow\; 0 \;\;, k_i \;\rightarrow\; 0 \;, i = \;1,..,4 \tag{2.6}$$

- Infra-red finiteness as an integral kernel i.e.

$$\int \frac{d^2k_1}{k_1^2}\frac{d^2k_2}{k_2^2}\delta^2(q-k_1-k_2)K^{(2)}_{2,2}(k_1,k_2,k_3,k_4) \qquad is \;\; finite \tag{2.7}$$

These two properties actually determine the relative magnitude of the three kinematic forms $K^{(2)}_1, K^{(2)}_2$, and $K^{(2)}_3$. It is very simple to demonstrate them diagrammatically. First we note two simple rules for obtaining the $k_i \rightarrow 0$ limit for any transverse momentum diagram.

- $k_i \rightarrow 0$ gives zero if the line carrying $k_i$ is the single line of a 1-2, 2-1, or 1-1 vertex.

- In general, $k_i \to 0$ gives the subdiagram obtained by removing the line carrying $k_i$.

As we outlined in [2] and discuss further in [5], the Ward identity constraint (2.6) should be satisfied by any reggeon amplitude in a gauge theory. It is easily proved diagrammatically. Using a dotted line to denote the $k_i$ line, we obtain the result shown in Fig. 2.3

Fig. 2.3 The Ward identity constraint for $K^2$

There is a subtlety in applying the first rule above. While the vertex involved carries a factor of $k_i^2$, if it is attached to a loop then the loop integral will have a threshold divergence. This divergence will produce an additional factor of $k_i^{-2} ln[k_i^2]$, apparently nullifying the Ward identity zero. However, if we regulate the loop integrals the vertex zero does give the requisite vanishing of the regulated integral. The cancellation of divergences then leads to the persistence of the zero in the unregulated kernel. We shall discuss this effect in the $O(g^4)$ kernel in the next Section. (The trajectory function appearing in $K_1^{(2)}$ is actually a prime example of this combination of a zero and a divergence. The effective persistence of the zero is then equivalent to the persistence of reggeization, i.e. that the gluon Regge trajectory passes through $\omega = 0$ at $k^2 = 0$.)

Note that the Ward identity actually determines the 2-2 vertex appearing in $K_3^{(2)}$ in terms of the 1-2 coupling appearing in $K_2^{(2)}$. In this way gauge invariance determines that the complete kernel is written in terms of a single coupling $g$, which can be identified with the gauge coupling, but in this context is more correctly identified as a three-reggeon coupling.

We make very little reference to color structure in this paper because we are discussing only physical kernels that carry zero ($t$-channel) color. In the $O(g^2)$ kernel the only remnant of the gauge group is then the overall normalization factor of $N$. The infra-red finiteness property is actually a zero color property. To demonstrate (2.7) diagrammatically we first note that infra-red divergences occur when the momentum

$k_i$ of an internal line vanishes. If we use a mass regulation then, as $m^2 \rightarrow 0$, this gives

$$\int d^2k_i \; f(k_i)/(k_i^2+m^2) \;\rightarrow\; \frac{1}{2}\int \frac{dk_i^2}{(k_i^2+m^2)} \int_0^{2\pi} d\theta \; f(0) \;\rightarrow\; \pi \; log[m^2] \; f(0) \qquad (2.8)$$

where (apart from a factor of $(16\pi^3)^{-1}$) $f(0)$ is obtained from the original diagram by removing the line carrying $k_i$.

The Ward identity constraint already determines that there is no divergence in (2.7) as $k_1 \rightarrow 0$ or $k_2 \rightarrow 0$ (for non-zero q). Potential divergences are therefore at $k_{1,2} = k_{3,4}$. The cancellation of infra-red divergences of this kind is demonstrated diagrammatically in Fig. 2.4.

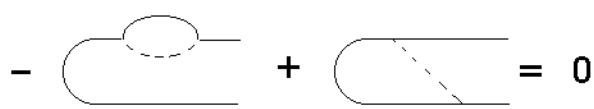


Fig. 2.4 Cancellation of infra-red divergences for $K^2$.

To find the $\omega$-plane singularities of $F(\omega, k, q-k)$ we project (2.3) on the complete set of orthogonal eigenfunctions

$$\phi_{\mu,n}(k) \;=\; (k^2)^{\mu} \; e^{in\theta} \qquad \mu = \frac{1}{2} + i\nu, \quad n = 0, \pm 1, \pm 2, ... \qquad (2.9)$$

where $k = (|k|cos\theta, |k|sin\theta)$. (Our definition of the kernel requires that we keep a factor of $k^{-2}$ in the measure of the completeness relation for eigenfunctions relative to [7]).

Note that when $k^2 \sim k'^2 \rightarrow \infty$, $K(k,k',q) \rightarrow K(k,k')$. Since this region contributes dominantly to the eigenvalue spectrum, the eigenvalues are independent of $q^2$ and take the form

$$\frac{Ng^2}{2\pi^2} \; \chi(\nu, n) \qquad (2.10)$$

where

$$\chi(\nu, n) \;=\; \psi(1) - Re\psi(\frac{|n|+1}{2} + i\nu) \qquad \nu \; \epsilon \; (-\infty, \infty), \quad n = 0, \pm 1, \pm 2, ... \quad (2.11)$$

with $\psi(x) = \frac{d}{dx}\Gamma(x)$. With $\tilde{F} = \delta^2(k-\tilde{k})$, the solution of (2.3) at $q=0$ is the reggeon Green function

$$F(k,\tilde{k}) = \sum_{n=-\infty}^{\infty} \frac{e^{in(\theta-\tilde{\theta})}}{4\pi^2} \int_{-\infty}^{\infty} \frac{d\nu \ \ (k^2/\tilde{k}^2)^{i\nu}}{\omega - \frac{Ng^2}{2\pi^2}\ \chi(\nu,n)} \tag{2.12}$$

The leading singularity in the $\omega$-plane is given by

$$\alpha_0 - 1 = \frac{Ng^2}{2\pi^2}\ \chi(0,0) \tag{2.13}$$

where $\chi(0,0)$ is the leading eigenvalue. If we write $\alpha_s = g^2/4\pi$ then since

$$\chi(0,0) = 2ln2 \tag{2.14}$$

we obtain from (2.13), the familiar result,

$$\alpha_0 - 1 = (\frac{12\alpha_s}{\pi})ln2 \ \sim \ -\frac{1}{2} \tag{2.15}$$

for the small-x power behaviour of parton distributions.

To discuss the conformal symmetry properties of the eigenvalue spectrum (2.11) we rewrite (2.11) as[6]

$$4\chi(\nu,n) = 4\psi(1) - \psi(m) - \psi(1-m) - \psi(\tilde{m}) - \psi(1-\tilde{m}) \tag{2.16}$$

where now

$$m = \frac{1}{2} + i\nu + \frac{n}{2}\ ,\ \tilde{m} = \frac{1}{2} + i\nu - \frac{n}{2}\ , \tag{2.17}$$

are conformal weights. $m(1-m)$ and $\tilde{m}(1-\tilde{m})$ are, respectively, the eigenvalues of the holomorphic and antiholomorphic Casimir operator of linear conformal transformations.

We can rewrite (2.16) as

$$4\chi(\nu,n) = \mathcal{F}[m(1-m)] + \mathcal{F}[\tilde{m}(1-\tilde{m})] \tag{2.18}$$

where using

$$\psi(x) = \psi(1) - \sum_{r=0}^{\infty}\Big(\frac{1}{r+x} - \frac{1}{r+1}\Big) \tag{2.19}$$

we find[6]

$$\mathcal{F}[x] \;=\; \sum_{r=0}^{\infty}\Big(\frac{2r+1}{r(r+1)\;+\;x} - \frac{2}{r+1}\Big) \tag{2.20}$$

That the eigenvalues can be written as a function of $m(1-m)$ plus a function of $\tilde{m}(1-\tilde{m})$ gives the holomorphic factorization of the kernel and the conformal symmetry of the BFKL equation[6].

## 3. THE $O(g^4)$ REGGEON KERNEL

We consider specifically the contribution of ($t$-channel) four-particle nonsense states to the $O(g^4)$ kernel. In Refs. [3, 4] we also considered the contribution obtained by iteration of the two-particle nonsense states. We will postpone discussion of this component until later Sections. It is the the interesting mathematical properties of the four-particle component with which we shall be mostly concerned in this paper. We study, therefore, the $O(g^4)$ kernel $K^{(4)}_{2,2}$ defined by the sum of transverse momentum integrals

$$\frac{1}{(g^2N)^2}K^{(4n)}_{2,2}(k_1,k_2,k_3,k_4) \;=\; K^{(4)}_0 \;+\; K^{(4)}_1 \;+\; K^{(4)}_2 \;+\; K^{(4)}_3 \;+K^{(4)}_4 \;. \tag{3.1}$$

with

$$K^{(4)}_0 \;=\; \frac{1}{2}\sum\; k_1^4k_2^4J_1(k_1^2)J_1(k_2^2)(16\pi^3)\delta^2(k_2-k_3)\;, \tag{3.2}$$

$$K^{(4)}_1 \;=\; -\frac{1}{3}\sum\; k_1^4J_2(k_1^2)k_2^2(16\pi^3)\delta^2(k_2-k_3) \tag{3.3}$$

$$K^{(4)}_2 \;=\; -\frac{1}{2}\sum\Big(\frac{k_1^2J_1(k_1^2)k_2^2k_3^2+k_1^2k_3^2J_1(k_4^2)k_4^2}{(k_1-k_4)^2}\Big), \tag{3.4}$$

$$K^{(4)}_3 \;=\; \frac{1}{2}\sum\; k_2^2k_4^2J_1((k_1-k_4)^2)\;, \tag{3.5}$$

and

$$K^{(4)}_4 \;=\; \frac{1}{4}\sum\; k_1^2k_2^2k_3^2k_4^2\;I(k_1,k_2,k_3,k_4), \tag{3.6}$$

where $J_1(k^2)$ is defined by (2.5) and

$$J_2(k^2) \;=\; \frac{1}{16\pi^3}\int d^2q \frac{1}{(k-q)^2} J_1(q^2) \quad , \tag{3.7}$$

and

$$I(k_1,k_2,k_3,k_4) \;=\; \frac{1}{16\pi^3}\int d^2p \frac{1}{p^2(p+k_1)^2(p+k_1-k_4)^2(p+k_3)^2}. \tag{3.8}$$

As for the $O(g^2)$ kernel, the only remnant of the color structure is in the normalization factor of $N^2$. We will show in [5] that the coefficients of the contributing $K_i^{(4)}$ and the absolute normalization of $K_{2,2}^{4n}$ are determined directly by $t$-channel unitarity, together with the color factors given by the group structure, apart from the ambiguity of the magnitude of the new 1-3 coupling appearing in $K_1^{(4)}$, $K_2^{(4)}$ and $K_3^{(4)}$. The diagrammatic representation of $\hat{K}_{2,2}^{4n}$ is shown in Fig. 3.1.

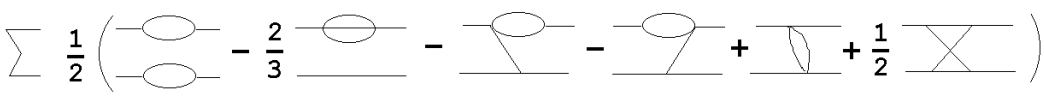


Fig. 3.1 The diagrammatic representation of $\hat{K}_{2,2}^{4n}$.

From this figure it is clear that the 1-3 vertex is the only new ingredient of the $O(g^4)$ kernel compared to the $O(g^2)$ kernel. It's magnitude is determined by the Ward Identity constraint that the kernel should vanish when $k_i \to 0,\ i = 1,..,4$.

Diagrammatically the Ward identity is satisfied as illustrated in Fig. 3.2

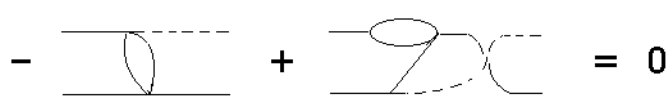


Fig. 3.2 The Ward identity constraint for $K^{4n}$.

and so determines the relative weight of $K_2^{(4)}$ and $K_3^{(4)}$. Although both diagrams contain the new 1-3 vertex, $K_3^{(4)}$ contains the square of this vertex, while $K_2^{(4)}$ contains

it singly together with the square of the 1-2 vertex. Therefore the Ward identity determines the new vertex in terms of the square of the 1-2 vertex.

There are two infra-red finiteness requirements following from the zero color of the kernel. These lead to three constraints, that determine the relative weights of the remaining components. First we require that the connected part of the kernel is infra-red finite before integration. This is illustrated in Fig. 3.3

Fig. 3.3 Infra-red finiteness of the connected part of $K^{4n}$.

and determines $K_4^{(4)}$ relative to $K_2^{(4)}$ and $K_3^{(4)}$. Taking the Ward identity zeroes into account, infra-red finiteness after integration requires cancellation, by the disconnected parts, of two divergences due to the connected part. First the poles of $K_2^{(4)}$ require the cancellation shown in Fig. 3.4.

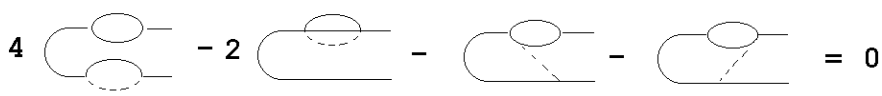


Fig. 3.4 Infra-red cancellation of the poles in $K_2^{(4)}$.

Secondly $K_3$ generates a divergence, when both exchanged lines carry zero transverse momentum, which requires the cancellation shown in Fig. 3.5.

Fig. 3.5 Infra-red cancellation of divergences due to $K_3^{(4)}$.

This last constraint determines $K_1^{(4)}$ relative to $K_2^{(4)} + K_3^{(4)} + K_4^{(4)}$ and the previous constraint then determines the relative weight of $K_0^{(4)}$.

In our original construction of $K^{(4n)}$ in [2], we particularly emphasized that the relative weights of all the terms in $K^{(4n)}$ are determined by the combination of the Ward identity constraint with the infra-red finiteness cancellations. However, as we stated above, we show in [5] that $t$-channel unitarity, together with the Ward identities and color factors, also determines all coefficients. Therefore infra-red finiteness can actually be deduced from $t$-channel unitarity, with the use of Ward identities, as might be anticipated.

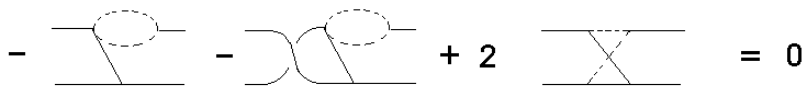


Fig. 3.6 Threshold cancellation in $K_2^{(4)}$ and $K_4^{(4)}$.

Finally we return to the issue of the interplay of multiplicative divergences and explicit Ward identity zeroes. $K_2^{(4)}$ contains diagrams with this problem. However, $K_4^{(4)}$ also has an explicit zero for each external line which is invalidated by threshold divergences. As illustrated in Fig. 3.6, after infra-red cancellations, the Ward identity is preserved by cancellation of the leading threshold behaviour of $K_2^{(4)}$ and $K_4^{(4)}$.

The most complicated part of $K^{(4n)}$ is clearly $K_4^{(4)}$ since it contains the box diagram i.e. a loop integral with four propagators. This diagram will actually occupy a major part of our remaining discussion. In the next Section we describe the explicit evaluation of the integral as a sum of logarithms.

## 4. EVALUATION OF THE BOX AS A SUM OF LOGARITHMS

Since $I(k_1, k_2, k_3, k_4)$ is an infra-red divergent integral, to obtain an explicit expression for it we first introduce a mass $m$ for each propagator. We then have a standard one-loop integral which appears in many two-dimensional field theories.

There are two basic ways of evaluating one loop n-point functions in two dimensions. According to ref. [8], in $D = 2$, form factors can be reduced to a sum of 3 self energy integrals, and, in general, an n-point function reduces to three $(n-1)$-point functions. The procedure can be applied iteratively until one is left only with

a set of self energy integrals, each of them giving one logarithm. In the case of the box diagram this method generates 9 logarithms (1 box $\rightarrow$ 3 form factors $\rightarrow$ 9 logs).

In principle one could also use the zero mode invariance of the decomposition of ref. [8] to reorganize the coefficients of the logarithms and so reduce their number, but in practice this can be tedious. Therefore, it is convenient to keep the number of logarithms as low as possible from the beginning. As the infra-red analysis of the previous Section shows, the box has 4 distinct infra-red divergences, each generating a logarithm as a mass singularity. However, as we shall see, a complete evaluation of the box involves, as a minimum, logarithms associated with all possible kinematic thresholds. A systematic method to evaluate this minimal number of logs has been developed long ago by Källen and Toll [9] and, later, in the analysis of the massive Thirring model, by Berg [10].

In this last method one propagator is set on shell by the first integration and a second is set on shell after partial fractioning. The second integration then generates a logarithm. The remaining parts of the diagram, the "trees", are factored out. The non-trivial part of the procedure is in fact the evaluation of the tree contributions. This is rather cumbersome and requires the introduction of dual momenta for the internal lines. In our application we have found it convenient to re-express these dual momenta in terms of the original momenta of the scattering diagram. We are then able to obtain explicit, if rather lengthy, expressions. We will present most of the details of our calculations in Appendices, but we can outline them as follows.

In order to apply the Källen and Toll[9] formalism directly we evaluate integrals in the timelike region. In fact with this formalism we obtain

$$\begin{aligned} 16\pi^3 J_1(k^2,m^2) &= \int d^2p \frac{1}{(p^2+m^2)((p-k)^2+m^2)} \\ &= \frac{i\pi}{\lambda^{1/2}(k^2,m^2,m^2)} Log\left(\frac{k^2-2m^2-\lambda^{1/2}(k^2,m^2,m^2)}{k^2-2m^2+\lambda^{1/2}(k^2,m^2,m^2)}\right). \end{aligned} \tag{4.1}$$

where now $\lambda^{1/2}(k^2,m^2,m^2) = \sqrt{k^2(k^2-4m^2)}$. (To agree directly with the analytic continuation from negative $k^2$ we should actually evaluate the two logarithms in (4.1) on different sheets. But since we are only interested in the real parts of integrals as $m^2 \rightarrow 0$, this is irrelevant for our purposes. This is discussed further in D.)

In order to discuss a planar box diagram we also, temporarily, interchange $k_1$

and $k_4$ and take all momenta to be flowing into the diagram. We therefore consider

$$\begin{aligned} I_4(k_1,k_2,k_3,k_4,m^2) &= 16\pi^3 I(k_4,k_2,-k_3,-k_1,m^2) \\ &= \int d^2p \frac{1}{[p^2-m^2][(p+k_1)^2-m^2][(p+k_1+k_2)^2-m^2][(p-k_4)^2-m^2]} \end{aligned} \tag{4.2}$$

We shall use the notation $p_i$, $(i = 1,..,4)$ for the internal momentum flowing along the $i$-th internal line, in addition to the loop momentum $p$, and defined such that if $p_{jk} = (p_j - p_k)^2$ then $p_{j,j+1} = k_j$ (with the obvious notation that $p_5 \equiv p_1$). This notation is illustrated in Fig. 4.1.

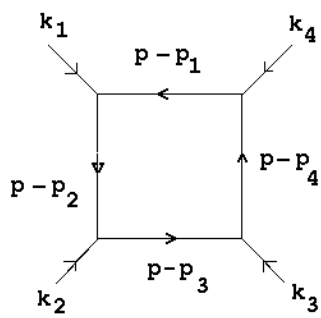


Fig. 4.1 Notation for the box diagram

There will be one logarithm in our result for each $p_{jk}$. In anticipation of this we define $X_{jk}$ by

$$X_{jk} = \frac{p_{jk}^2 - 2m^2 - \lambda^{1/2}(p_{jk}^2, m^2, m^2)}{p_{jk}^2 - 2m^2 + \lambda^{1/2}(p_{jk}^2, m^2, m^2)} \tag{4.3}$$

and write

$$F_{jk} \equiv F(p_{jk}^2, m^2) = \frac{i\pi}{\lambda^{1/2}(p_{jk}^2, m^2, m^2)} Log X_{jk}. \tag{4.4}$$

We similarly identify trees $A_{jk}$ by the indices of the lines which have been set on shell. This is illustrated in Fig. 4.2.

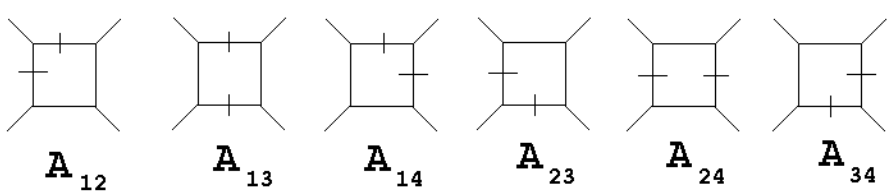

Fig. 4.2 Tree diagrams obtained by putting on-shell the crossed lines.

To evaluate the trees, we need an explicit expression for the loop momentum $p$ which satisfies

$$\begin{aligned}(p-p_j)^2-m^2&=0\\(p-p_k)^2-m^2&=0.\end{aligned}\tag{4.5}$$

These two conditions are solved in [9] by the vectors

$$p=q^{\pm}_{jk}=\frac{1}{2}\left(p_j+p_k\pm p^d_{kj}\frac{\lambda^{1/2}(p^2_{jk},m^2,m^2)}{p^2_{jk}}\right).\tag{4.6}$$

where we have introduced dual vectors $p^d$ satisfying the conditions

$$p^d{}_{jk}\cdot p_{jk}=0,\quad p^{d^2}_{jk}=-p_{jk}{}^2\tag{4.7}$$

Since $p_{j,j+1}=k_j$, we can go one step further compared to [9] by noticing that the dual momenta can be expressed in terms of momenta that are simply (dual) orthogonal to the external lines. In particular we can take

$$\begin{aligned}k^d{}_1&=\frac{\epsilon(n_{12})}{\sqrt{(k_1\cdot k_2)^2-k_1^2k_2^2}}\left(k_1k_1\cdot k_2-k_2k_1^2\right)\\k^d{}_2&=\frac{\epsilon(n_{21})}{\sqrt{(k_1\cdot k_2)^2-k_1^2k_2^2}}\left(k_2k_1\cdot k_2-k_1k_2^2\right)\\k^d{}_3&=\frac{\epsilon(n_{34})}{\sqrt{(k_3\cdot k_4)^2-k_3^2k_4^2}}\left(k_3k_3\cdot k_4-k_4k_3^2\right)\\k^d{}_4&=\frac{\epsilon(n_{43})}{\sqrt{(k_3\cdot k_4)^2-k_3^2k_4^2}}\left(k_3k_3\cdot k_4-k_4k_3^2\right),\end{aligned}\tag{4.8}$$

where we have defined

$$n_{12}=k_1^1k_2^0-k_1^0k_2^1\ ,\qquad n_{34}=k_3^1k_4^0-k_3^0k_4^1\ ,\tag{4.9}$$

and $n_{21} = -n_{12}$, $n_{34} = -n_{43}$. $\epsilon(x) = \theta(x) - \theta(-x)$ is the sign function. We have the relations

$$\begin{aligned} n_{12} &= \sqrt{(k_1 \cdot k_2)^2 - k_1^2 k_2^2} = \sqrt{\lambda(s, k_1^2, k_2^2)} \\ n_{12} &= \sqrt{(k_3 \cdot k_4)^2 - k_3^2 k_4^2} = \sqrt{\lambda(s, k_3^2, k_4^2)} \end{aligned} \tag{4.10}$$

We now define

$$A_{jk} = \frac{1}{2}\left(A^{+}{}_{jk} + A^{-}{}_{jk}\right). \tag{4.11}$$

where

$$\frac{1}{A^{\pm}_{jk}} = \prod_{l \neq j,k} \left((q^{\pm}_{jk} - p_l)^2 + m^2\right) \tag{4.12}$$

In a general n-point function the product in (4.12) would run over the $n-2$ propagators which are left off-shell. Then the full expression for an n-point diagram (here denoted by $I_n$) is given by

$$I_n = \sum_{j\,<\,k} A_{jk} F_{jk}. \tag{4.13}$$

including, of course, $n = 4$. The number of coefficients generated is $n(n-1)/2$ for an $n$-point function.

In the specific case of the planar box diagram this method gives (to simplify the evaluation for the next Section we take $k_3$ and $k_4$ to be flowing out)

$$\begin{aligned} & I_4(k_1, k_2, k_3, k_4) \quad \Big( \equiv \; I(-k_4, k_2, k_3, -k_1) \Big) \\ &= \; A_{12} F\left(k_3^2, m^2\right) + A_{13} F\left((k_1 + k_2)^2, m^2)\right) + A_{14} F\left(k_4^2, m^2\right) \\ &\quad + A_{23} F\left(k_2^2, m^2\right) + A_{24} F\left((k_2 - k_3)^2, m^2\right) + A_{34} F\left(k_1^2, m^2\right) \end{aligned} \tag{4.14}$$

where F is given by (4.4).

Further discussion of the the results with $m^2$ kept finite can be found in the Appendix. Clearly in the limit $m^2 \to 0$ only the $X_{jk}$ are divergent. The trees, i.e. the $A_{jk}$ simplify considerably and we give examples of their complete expression here. Note that although the $A^{\pm}_{j,k}$ are initially defined separately as a product of

simple denominators, combining them leads to relatively complicated expressions. For convenience we define

$$A_{ij} = \frac{a_{ij}}{b_{ij}} \tag{4.15}$$

Examples of the $a_{ij}$ and $b_{ij}$ are

$$\begin{aligned} a_{12} = \quad & \Big[k_1 \cdot {k_2}^2 - {k_1}^2\, {k_2}^2\Big] \\ & \times\Big[k_1 \cdot {k_2}^2 - k_1 \cdot k_2\, k_1 \cdot k_3 - {k_1}^2\, {k_2}^2 + {k_1}^2\, k_2 \cdot k_3 \\ & +(k_1 \cdot k_2 + {k_2}^2)\,(k_1 \cdot k_2 - k_1 \cdot k_3 + {k_2}^2 - 2\, k_2 \cdot k_3 + {k_3}^2)\Big] \end{aligned} \tag{4.16}$$

$$\begin{aligned} b_{12} = \quad & \Big[-k_1 \cdot {k_2}^2 + {k_1}^2\, {k_2}^2 + (k_1 \cdot k_2 + {k_2}^2)^2\Big] \\ & \times \Big[-(k_1 \cdot {k_2}^2 - k_1 \cdot k_2\, k_1 \cdot k_3 - {k_1}^2\, {k_2}^2 + {k_1}^2\, k_2 \cdot k_3)^2 \\ & +(k_1 \cdot {k_2}^2 - {k_1}^2\, {k_2}^2))\,(k_1 \cdot k_2 - k_1 \cdot k_3 + {k_2}^2 - 2\, k_2 \cdot k_3 + {k_3}^2)^2\Big] \end{aligned} \tag{4.17}$$

$$\begin{aligned} a_{23} = \quad & \Big[k_1 \cdot {k_2}^2 - {k_1}^2\, {k_2}^2\Big] \\ & \times\Big[-(k_1 \cdot k_3\, {k_2}^2) + k_1 \cdot k_2\, k_2 \cdot k_3 + ({k_1}^2 + k_1 \cdot k_2)\,(-k_2 \cdot k_3 + {k_3}^2)\Big] \end{aligned} \tag{4.18}$$

$$\begin{aligned} b_{23} = \quad & \Big[-k_1 \cdot {k_2}^2 + ({k_1}^2 + k_1 \cdot k_2)^2 + {k_1}^2\, {k_2}^2\Big] \\ & \times\Big[-[-(k_1 \cdot k_3\, {k_2}^2) + k_1 \cdot k_2\, k_2 \cdot k_3]^2 + (k_1 \cdot {k_2}^2 - {k_1}^2\, {k_2}^2)\,(-k_2 \cdot k_3 + {k_3}^2)^2\Big] \end{aligned} \tag{4.19}$$

$$\begin{aligned} a_{34} = \quad & \Big[k_3 \cdot {k_4}^2 - {k_3}^2\, {k_4}^2\Big]\ \Big[\Big([-k_2 \cdot k_4\, {k_3}^2 + k_2 \cdot k_3\, k_3 \cdot k_4]\,[-(k_1 \cdot k_4 + k_2 \cdot k_4)\, {k_3}^2 \\ & +(k_1 \cdot k_3 + k_2 \cdot k_3)\, k_3 \cdot k_4]) + \Big((k_2{}^2 - k_2 \cdot k_3)\,({k_1}^2 + 2\, k_1 \cdot k_2 - k_1 \cdot k_3 \\ & +{k_2}^2 - k_2 \cdot k_3)\,(k_3 \cdot {k_4}^2 - {k_3}^2\, {k_4}^2)\Big)\Big] \end{aligned} \tag{4.20}$$

The remaining $a_{ij}$ and $b_{ij}$ are given in Appendix B.

Since $K_2^{(4)}$ and $K_3^{(4)}$ involve only $J_1$ it is clear that by utilising (4.1), (4.3), (4.4) and (4.14) and taking the $m^2 \to 0$ limit in all logarithms, we can obtain an analytic expression for the the full connected part of the kernel. We will not write it out in full. Instead we proceed directly to the forward kernel which is very much simpler. We also will not consider the full disconnected part here. We will discuss this explicitly for the case of the forward kernel in the next Sections.

## 5. THE $O(g^4)$ PARTON KERNEL

As we have discussed in Section 2, it is the forward kernel $K_{2,2}^{(4n)}(q-k,k,k',q-k')$ which appears in the parton evolution equation. To evaluate the contribution of $K_4^{(4)}$ we require $I(k,k') = I_4(k',k,k',k)$. The simplification of the $X_{jk}$ as $m^2 \to 0$ gives

$$\begin{aligned} 4\pi^2 I[k,k'] = & \frac{A_{12}}{k'^2} Log[k'^2/m^2] + \frac{A_{23}}{k^2} Log[k^2/m^2] + \frac{A_{34}}{k'^2} Log[k'^2/m^2] \\ & + \frac{A_{13}}{(k+k')^2} Log[(k+k')^2/m^2] + \frac{A_{14}}{k^2} Log[k^2/m^2] + \frac{A_{24}}{(k-k')^2} Log[(k-k')^2/m^2] \end{aligned} \tag{5.1}$$

The complicated expressions for the $A_{jk}$ given in the previous Section simplify enormously when $q = 0$ and we obtain

$$\begin{aligned} A_{12} &= \frac{k^2 - k'^2}{k^2(k+k')^2(k-k')^2} & A_{13} &= \frac{1}{k^2 k'^2} \\ A_{14} &= \frac{k'^2 - k^2}{k'^2(k+k')^2(k-k')^2} & A_{23} &= \frac{k'^2 - k^2}{k'^2(k+k')^2(k-k')^2} \\ A_{24} &= \frac{1}{k^2 k'^2} & A_{34} &= \frac{k^2 - k'^2}{k^2(k+k')^2(k-k')^2} \end{aligned} \tag{5.2}$$

Note that the $m^2$ divergences multiplying $A_{23}$ and $A_{14}$, and $A_{34}$ and $A_{12}$ cancel pairwise. The remaining divergences have to cancel with the remaining terms of the kernel.

From (5.1) and (5.2) we have that, as $m^2 \to 0$,

$$K_4^{(4)} \;\to\; \frac{-\,k^2k'^2}{8\pi^2}\Bigg(\frac{2(k'^2-k^2)}{(k+k')^2(k-k')^2}Log\left[\frac{k'^2}{k^2}\right] + \frac{1}{(k-k')^2}Log\left[\frac{(k-k')^2}{m^2}\right] \;+\; \frac{1}{(k+k')^2}Log\left[\frac{(k+k')^2}{m^2}\right]\Bigg)\;. \tag{5.3}$$

$K_3^{(4)}$ simply gives a contribution of the same form as the last two terms in (5.3), i.e. as $m^2 \to 0$

$$\tilde{K}_3 \;\to\; \frac{k^2k'^2}{8\pi^2}\left(\frac{1}{(k-k')^2}Log\left[\frac{(k-k')^2}{m^2}\right] + \frac{1}{(k+k')^2}Log\left[\frac{(k+k')^2}{m^2}\right]\right) \tag{5.4}$$

Similarly $K_2^{(4)}$ gives

$$\tilde{K}_2 \to \frac{-k^2k'^2}{8\pi^2}\Bigg(\frac{1}{(k-k')^2}(Log\left[\frac{k^2}{m^2}\right] + Log\left[\frac{k'^2}{m^2}\right]) + \frac{1}{(k+k')^2}(Log\left[\frac{k^2}{m^2}\right] + Log\left[\frac{k'^2}{m^2}\right])\Bigg). \tag{5.5}$$

The infra-red finiteness of the connected part $K_c^{(4n)} \;=\; K_2^{(4)} + K_3^{(4)} + K_4^{(4)}$ is now apparent and we can write

$$\begin{aligned} K_c^{(4n)} \;&=\; \frac{1}{8\pi^2}\left(\frac{k^2k'^2}{(k-k')^2}Log\left[\frac{(k-k')^4}{k^2k'^2}\right] \;+\; \frac{k^2k'^2}{(k+k')^2}Log\left[\frac{(k+k')^4}{k^2k'^2}\right]\right) \\ &\quad -\quad \left(\frac{2k^2k'^2(k^2-k'^2)}{(k-k')^2(k+k')^2}Log\left[\frac{k^2}{k'^2}\right]\right) \\ &=\quad \Big(\;\mathcal{K}_1\;\Big) \;-\; \Big(\;\mathcal{K}_2\;\Big). \end{aligned} \tag{5.6}$$

Only $\mathcal{K}_1$ gives infra-red divergences (at $k' = \pm k$) when integrated over $k'$. The infra-red analysis of Section 3 showed that these divergences are cancelled by $K_0$ and $K_1$. (Note that the normalization of $\mathcal{K}_1$ and $\mathcal{K}_2$ differs from that in [4].)

We emphasized in [4] that $\mathcal{K}_2$ has a number of attractive properties which make it interesting to study separately and we shall see this in the following. However, we

should also note the following inter-relation between the two components. If we consider the limit $k^2 \to 0$ we find

$$\mathcal{K}_1 \;\to\; \frac{k^2}{4\pi^2} Log\left[\frac{k'^2}{k^2}\right] \quad , \qquad\qquad \mathcal{K}_2 \;\to\; -\frac{k^2}{4\pi^2} Log\left[\frac{k'^2}{k^2}\right] \quad , \tag{5.7}$$

and so there is a cancellation between $\mathcal{K}_1$ and $\mathcal{K}_2$. This cancellation is a consequence of the Ward identity cancellation between $K_2^{(4)}$ and $K_4^{(4)}$ discussed in Section 3 and illustrated by Fig. 3.6. Consequently the Ward identity property relates $\mathcal{K}_1$ and $\mathcal{K}_2$ even though their infra-red properties allow them to be separated.

Apart from the logarithmic factors, $\mathcal{K}_1$ has the same structure as the forward (connected) $O(g^2)$ kernel. Indeed, we now show that it is directly related to the square of the $O(g^2)$ kernel, evaluated in the forward direction. We show that (in the forward direction)

$$\hat{\mathcal{K}}_0 \;+\; \hat{\mathcal{K}}_1 \;=\; \frac{1}{4}\left(\hat{K}_{2,2}^{(2)}\right)^2 , \tag{5.8}$$

where $\mathcal{K}_0$ represents the sum of the disconnected parts $K_0^{(4)}$ and $K_1^{(4)}$. (5.8) will provide a simple determination of the eigenvalue spectrum of $\mathcal{K}_0 \;+\; \mathcal{K}_1$.

We derive (5.8) diagrammatically. The full square of $\hat{K}_{2,2}^{(2)}$ is given in Fig. 5.1.

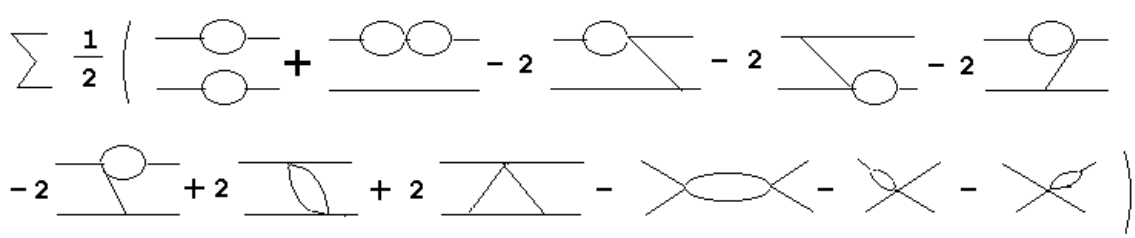


Fig. 5.1 The full square of $\hat{K}_{2,2}^{(2)}$

In the forward direction various distinct diagrams become equal. This is shown in Fig. 5.2.

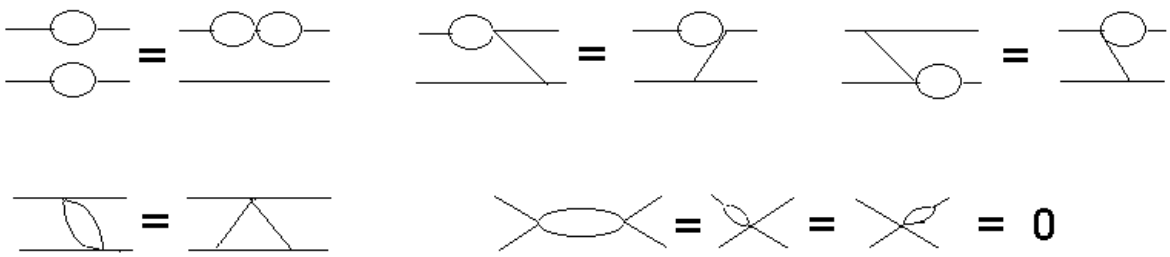


Fig. 5.2 Equalities in the forward direction.

and so $(\hat{K}^{(2)}_{2,2})^2$ simplifies to the result shown in Fig. 5.3.

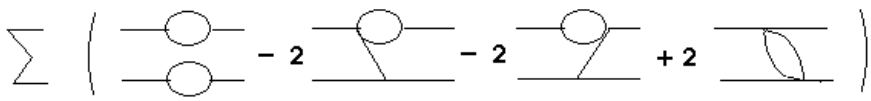


Fig. 5.3 Representation of $(\hat{K}^{(2)}_{2,2})^2$ in the forward direction.

From this we see that if we utilise (5.4) and (5.5), then (5.8) holds apart from the contribution of the disconnected parts. However, in Appendix D we show, using the dimensional regularization which we discuss just below, that

$$4k^2[J_2(k^2)] \;=\; 3[k^2 J_1(k^2)]^2$$

and this is sufficient to show that (5.8) is also valid when the disconnected parts are included.

To introduce a complete dimensionally regularized form for $K^{(4n)}(k,k')$ we replace each $Log[k^2]$ using the dimensionally regularized form of $J_1(k^2)$, i.e.

$$Log[k^2] \;=\; 8\pi^2 J_1(k^2) \;=\; \frac{k^2}{2\pi}\int \frac{d^D q}{q^2(k-q)^2} \;=\; \eta[k^2]^{D/2\,-1} \tag{5.9}$$

where

$$\eta = \frac{\Gamma[2-D/2]\Gamma[D/2-1]^2}{2\Gamma[D-2]} \underset{D\,\to\,2}{\longrightarrow} \frac{2}{(D-2)} \tag{5.10}$$

Notice that this is possible (in $D = 2 + \epsilon$ dimensions) *only* because we have shown the cancellation of the mass singularities in eq. 5.6. In fact, in the limit of $\epsilon \to 0$, a suitable choice of the dimensional regularization scale $\mu$ allows us to reproduce the same expressions for the components of the kernel regulated by a cutoff $m$.

We can then write the complete normalised kernel in D dimensions as

$$\frac{1}{(g^2N)^2}K^{(4n)} \;=\; \Big(\;\mathcal{K}_0\;\Big) \;+\; \Big(\;\mathcal{K}_1\;\Big) \;-\; \Big(\;\mathcal{K}_2\;\Big), \tag{5.11}$$

where now

$$\mathcal{K}_0 \;=\; \frac{1}{8\pi}\eta^2(k^2)^D\Big(\delta^2(k-k') + \delta^2(k-k')\Big) \tag{5.12}$$

$$\begin{aligned}\mathcal{K}_1 \;=\; \frac{\eta}{8\pi^2}\Big(&2k^2k'^2([(k'-k)^2]^{D/2-2} \;+\; [(k+k')^2]^{D/2-2}) \\ &-(k^2[k'^2]^{D/2} \;+\; [k^2]^{D/2}k'^2)(\frac{1}{(k'-k)^2} \;+\; \frac{1}{(k'+k)^2})\Big)\end{aligned} \tag{5.13}$$

and

$$\mathcal{K}_2 \;=\; \frac{\eta}{4\pi^2}\;\frac{k^2k'^2(k^2-k'^2)}{(k+k')^2(k-k')^2}\left((k^2)^{D/2\;-1} - (k'^2)^{D/2\;-1}\right). \tag{5.14}$$

## 6. IMPACT PARAMETER REPRESENTATION

In this Section we give impact parameter repesentations, for components of the forward kernel, that we anticipate will be useful in further studies. In particular with respect to conformal symmetry and holomorphic factorization properties. We limit our discussion to the dimensionally regulated form of the kernel (in $D = 2 + \epsilon$ dimensions) and do not specialize our results to $D = 2$.

The expression for $\mathcal{K}_1(x, y)$ turns out to be much simpler than the corresponding expression for $\mathcal{K}_2(x, y)$, which can be written down in terms of a Gegenbauer expansion. For this purpose we have used a generalized expression for a 3-point function given in ref. [11], and which is briefly described in Appendix F. The Gegenbauer expansion is a particular case of the general result given in [11], and can be derived quite simply by expanding euclidean propagators (in $D$-dimensions) in the base of Gegenbauer polynomials [12].

We define

$$\mathcal{K}_1(x,y) \equiv \frac{1}{(2\pi)^{2D}} \int d^D\, k\, d^D\, k'\, e^{ik\cdot x} e^{ik\cdot y} \mathcal{K}_1(k,k').$$

It is convenient to also define

$$g_1(k,k') = \frac{2k^2 k'^2}{[(k'-k)^2]^{2-D/2}}\ , \qquad g_2(k,k') = \frac{k^2[k'^2]^{D/2}}{(k'-k)^2}\ , \tag{6.1}$$

and let $g_1(x,y)$ and $g_2(x,y)$ denote their corresponding expressions in impact parameter space. Noting that $g_1(x,y)$ is defined only in a distributional sense, we can write

$$\begin{aligned}\mathcal{K}_1(x,y) = \frac{\eta}{8\pi^2}\,&(g_1(x,y) + g_1(x,-y) \\ &-(g_2(x,y) + g_2(y,x)) - (g_2(-x,y) + g_2(-y,x)))\end{aligned} \tag{6.2}$$

and show that to $O(1/\epsilon)$

$$\frac{\eta}{8\pi^2}(g_1(x,y) + g_1(x,-y)) + \mathcal{K}_0(x,y) = 0 \tag{6.3}$$

As an explicit expression for $g_2(x,y)$ we can write

$$g_2(x,y) = \frac{-2^{D-2}}{\pi^D}\frac{\Gamma[D]\Gamma[D/2-1]}{\Gamma[-D/2]}\Box_x \frac{1}{[x_+^2]^D[x^2]^{D/2-1}}. \tag{6.4}$$

where $\Box_x \equiv \frac{\partial}{\partial_\mu}\frac{\partial}{\partial^\mu}$ . and

$$x_+ = x + y, \qquad x_- = x - y. \tag{6.5}$$

For $\mathcal{K}_2$ we can obtain a more complete expression. We write

$$\mathcal{K}_2(x,y) = \frac{\eta}{4\pi^2}\,(f_1(x,y) - f_2(x,y) + f_1(y,x) - f_2(y,x)) \tag{6.6}$$

with $f_1(x,y)$ and $f_2(x,y)$ being, respectively, the impact parameter representations of

$$f_1(k,k') = \frac{k'^2[k^2]^{D/2+1}}{(k+k')^2(k-k')^2}\ , \qquad f_2(k,k') = \frac{[k'^2]^2[k^2]^{D/2}}{(k+k')^2(k-k')^2}\ . \tag{6.7}$$

We obtain

$$f_1(x,y) = -\frac{1}{\pi^{3D/2}}\frac{\Gamma[D/2-1]^2\Gamma[D+1]}{\Gamma[-D/2-1]}2^{3D-6}\Box_y Y(D+1, D/2-1, D/2-1|x_+, x_-) \tag{6.8}$$

and

$$f_2(x,y) = \frac{1}{\pi^{3D/2}}\frac{\Gamma[D/2-1]^2\Gamma[D]}{\Gamma[-D/2]}2^{3D-8}(\Box_y)^2 Y(D, D/2-1, D/2-1|x_+, x_-) \tag{6.9}$$

where

$$Y(\sigma_1,\sigma_2,\sigma_3|x_+,x_-) = \int \frac{d^D\ z_1}{[z_1^2]^{\sigma_1}[(x_+ + z_1)^2]^{\sigma_2}[(x_- + z_1)^2]^{\sigma_3}} \tag{6.10}$$

is a generalized vertex function in impact parameter space.

In ref. [11] it is shown that eq. (6.10) can be re-expressed in terms of a Mellin-Barnes transform

$$\begin{aligned} Y(\sigma_1,\sigma_2,\sigma_3,x_+,x_-) &= \frac{\pi^{D/2} i^{1-D}[x_+^2]^{D/2-\sigma_1-\sigma_2-\sigma_3}}{(2\pi i)^2\Gamma[\sigma_1]\Gamma[\sigma_2]\Gamma[\sigma_3]\Gamma[D-\sigma_1-\sigma_2-\sigma_3]4\pi^2} \\ &\times \int_{-i\infty}^{i\infty}\int_{-i\infty}^{i\infty} dsdt\mathcal{X}^s\mathcal{Y}^t\Gamma[-s]\Gamma[-t] \\ &\times\Gamma[D/2-\sigma_1-\sigma_3-t]\Gamma[\sigma_3+s+t]\Gamma[\sigma_1+\sigma_2+\sigma_3-D/2+s+t), \end{aligned} \tag{6.11}$$

with

$$\mathcal{X} = \frac{4y^2}{x_+^2}, \quad \mathcal{Y} = \frac{x_-^2}{x_+^2}, \tag{6.12}$$

and the final result expressed in terms of generalized hypergeometric functions (Appel functions) of two variables $\mathcal{X},\ \mathcal{Y}$ (see ref. ([11])

$$F_4\left[a,b,c,d|\mathcal{X},\mathcal{Y}\right] = \sum_{j=0}^{\infty}\sum_{l=0}^{\infty}\frac{\mathcal{X}^j\mathcal{Y}^l(a)_{j+l}(b)_{j+l}}{j!\ l!\ \ (c)_j(d)_l} \tag{6.13}$$

and

$$(a)_j = \frac{\Gamma[a+j]}{\Gamma[j]} \tag{6.14}$$

denotes the Pochhammer symbol.

In our case, however, we can proceed in an alternative way. In the particular case $\sigma_2 = \sigma_3 = D/2 - 1 \equiv \lambda$, $Y$ can be rewritten as a Gegenbauer expansion. For this purpose we introduce the Gegenbauer polynomials

$$\begin{aligned} C_n^\lambda(x) &= \frac{(-2)^{-n}(1-x^2)^{-\lambda+1/2}\Gamma[n+2\lambda]\Gamma[\lambda+1/2]}{n!\Gamma[2\lambda]\Gamma[\lambda+1/2+n]}\frac{d^n}{dx^n}(1-x^2)^{n+\lambda-1/2} \\ &= \sum_{k=0}^{[n/2]} \frac{(-1)^k\Gamma[\lambda+n-k](2x)^{n-2k}}{k!(n-2k)!\Gamma[\lambda]} \end{aligned} \tag{6.15}$$

($[n/2]$ denotes the integer part of $n/2$) and by using the formulas in Appendix F we obtain

$$Y(\sigma_1, D/2-1, D/2-1|x_+, x_-) = \frac{2\pi^{\lambda+1}}{\Gamma[\lambda+1]}\frac{\lambda}{\lambda+n}\sum_n C_n^\lambda(\hat{x}_+\cdot\hat{x}_-)\mathcal{J}_n(x_+, x_-), \tag{6.16}$$

where we have defined $\hat{x} \equiv x^\mu/x^2$. An expression for $\mathcal{J}_n(x_+, x_-)$ can be found in the Appendix.

## 7. SPECTRUM OF THE PARTON KERNEL

In this Section we present results regarding the spectrum of the forward kernel. We use the complete set of orthogonal eigenfunctions, $\phi_{\mu,n}$, defined in (2.9). From (5.8), it follows that the eigenvalue spectrum of $\mathcal{K}_0 + \mathcal{K}_1$ is simply

$$\frac{1}{\pi}[\chi(\nu, n)]^2 \tag{7.1}$$

where, again $\mu = 1/2 + i\nu$, and $\chi(\nu, n)$ is given by (2.11). If we write $\Lambda(\nu, n)$ for the eigenvalues of $\mathcal{K}_2$ then the complete spectrum of $\hat{K}^{(4n)}$ is given by $N^2g^4\mathcal{E}(\nu, n)$ with

$$\mathcal{E}(\nu, n) = \frac{1}{\pi}[\chi(\nu, n)]^2 - \Lambda(\nu, n) . \tag{7.2}$$

The reggeon Green function solution of (2.3) with $K^{(4n)}$ added to the BFKL kernel $K^{(2)}$ is, when $q = 0$, a simple modification of (2.12) i.e.

$$F(k, k') = \sum_{n=-\infty}^{\infty} \frac{e^{in(\theta-\theta')}}{4\pi^2}\int \frac{d\nu \ (k^2/k'^2)^{i\nu}}{\omega - \frac{Ng^2}{2\pi^2}\chi(\nu, n) - \frac{N^2g^4}{16\pi^3}\mathcal{E}(\nu, n)} \tag{7.3}$$

To evaluate the spectrum of $\mathcal{K}_2$ we write

$$\begin{aligned}\mathcal{K}_2 \otimes \phi_{\mu,n} &= \mathcal{K}_2^1 \otimes \phi_{\mu,n} - \mathcal{K}_2^2 \otimes \phi_{\mu,n} \\ &= \lambda_1(\mu,n)\phi_{\mu,n} - \lambda_2(\mu,n)\phi_{\mu,n} \\ &= \lambda(\mu,n)\phi_{\mu,n}, \end{aligned} \tag{7.4}$$

where

$$\mathcal{K}_2^1 \otimes \phi_{\mu,n} = \frac{\eta}{4\pi^2}\int \frac{d^D k'}{(k'^2)^2}\frac{(k^2)^{D/2}k'^2(k^2-k'^2)\phi_{\mu,n}(k')}{(k-k')^2(k+k')^2,} \tag{7.5}$$

and

$$\mathcal{K}_2^2 \otimes \phi_{\mu,n} = \frac{\eta}{4\pi^2}\int \frac{d^D k'}{(k'^2)^2}\frac{k^2(k'^2)^{D/2}(k^2-k'^2)\phi_{\mu,n}(k')}{(k-k')^2(k+k')^2.} \tag{7.6}$$

We embed the eigenfunctions in a D-dimensional angular space parameterized by $(\theta_1, \theta_2, ..., \theta_{D-1})$ by assuming that $\theta \equiv \theta_{D-1}$. The only non trivial angular integral is then the following one (for simplicity we write $\theta_{D-1} \equiv \theta$)

$$\begin{aligned} I_\chi[n] &\equiv \int_0^{2\pi} d\theta \frac{e^{in\theta}}{1 - z(k,k')sin^2\ (\theta-\chi)} \\ z[k,k'] &= -\frac{4k^2k'^2}{(k^2-k'^2)^2} \end{aligned} \tag{7.7}$$

where $cos\chi = k\cdot\hat{x}$ and $cos\theta = k'\cdot\hat{x}$. We turn the angular integral into a complex line integral on the circle and we get by residui (for $n > \ -1$)

$$\begin{aligned} I_\chi[n] &= -4ie^{in\chi}\oint dw \frac{w^{n+1}}{zw^4 + 2(2-z)w^2 + z} \\ &= \quad 2\pi\delta_{n,2M}e^{in\chi}\left(\frac{k^2-k'^2}{k^2+k'^2}\right)\left[\left(\frac{k}{k'}\right)^n \Theta[k'-k] - \left(\frac{k'}{k}\right)^n \Theta[k-k']\right]. \end{aligned} \tag{7.8}$$

$2M$ here is an even integer - this will be important in the following. For $n < -1$ the integral has additional poles, however it is easy to show that $I[-n] = I[n]$ for any integer $n$. The remaining radial integral (in $k'^2$) is therefore symmetric for $n \to -n$.

$I_\chi[n]$ is symmetric under the exchange of $k$ and $k'$, and also is invariant under $k \to 1/k,\ k' \to 1/k'$. This last invariance is sufficient to show from (7.5) and (7.6) that

$$\lambda(\mu\ ,n) \ = \ \lambda(1-\mu\ ,n) \tag{7.9}$$

Using (7.8) we obtain from (7.5) and (7.6) that, as $D \to 2$,

$$\lambda_1(\mu,n) \;\to\; \frac{\eta}{4\pi^2}\frac{\pi^{D/2}}{\Gamma[D/2]}\Big(\beta(|n|/2+D/2+\mu-1) \;-\; \beta(|n|/2-D/2-\mu+2)\Big), \tag{7.10}$$

and

$$\lambda_2(\mu,n) \;\to\; \frac{\eta}{4\pi^2}\frac{\pi^{D/2}}{\Gamma[D/2]}\Big(\beta(|n|/2+D+\mu-2) \;-\; \beta(|n|/2-D-\mu+3)\Big), \tag{7.11}$$

where $\beta(x)$ is the incomplete beta function, i.e.

$$\begin{aligned}\beta(x) \;&=\; \int_0^1 dy\; y^{x-1}[1+y]^{-1} \\ &=\; \frac{1}{2}\Big(\psi(\frac{x+1}{2}) - \psi(\frac{x}{2})\Big),\end{aligned} \tag{7.12}$$

$\lambda_1(\mu,n)$ and $\lambda_2(\mu,n)$ are separately singular at $D=2$, but $\lambda(\mu,n)$ is finite, and writing $\Lambda(\nu,n) \;\equiv\; \lambda(\frac{1}{2}+i\nu\;,n)$, we obtain

$$\Lambda(\nu,n) \;=\; -\;\frac{1}{4\pi}\Big(\beta'(\frac{|n|+1}{2}+i\nu) \;+\; \beta'(\frac{|n|+1}{2}-i\nu)\Big). \tag{7.13}$$

Since

$$\beta'(x) \;=\; \frac{1}{4}\Big(\psi'(\frac{x+1}{2}) - \psi'(\frac{x}{2})\Big), \tag{7.14}$$

and

$$\psi'(z) \;=\; \sum_{r=0}^{\infty}\frac{1}{(r+z)^2}, \tag{7.15}$$

it follows that $\beta'(x)$ is a real analytic function and so, from (7.13), the eigenvalues $\Lambda(\nu,n)$ are all real.

We can also show from (7.13) that the eigenvalues $\Lambda(\nu,n)$ have the same holomorphic factorization property that we discussed for the leading order eigenvalues $\chi(\nu,n)$ in Section 2. That is we can write

$$\Lambda(\nu,n) \;=\; \mathcal{G}[m(1-m)] \;+\; \mathcal{G}[\tilde{m}(1-\tilde{m})] \tag{7.16}$$

where, as in Section 2, $m = 1/2+i\nu+n/2$ and $\tilde{m} = 1/2+i\nu-n/2$. We anticipate that, for the full kernel, the eigenvalues are independent of $q^2$ in analogy with the

$O(g^2)$ eigenvalues (because of the same dominance of large $k^2 \sim k'^2$). In this case, the spectrum we have obtained already determines the holomorphic factorization[6] and conformal symmetry properties of the non-forward kernel.

We can rewrite (7.13) as

$$\begin{aligned}
16\pi\Lambda(\nu,n) \;&=\; -\;4\Big(\beta'(m)\;+\;\beta'(1-\tilde{m})\Big)\\
&= \psi'\Big(\frac{m+1}{2}\Big)\;-\;\psi'\Big(\frac{m}{2}\Big)\;+\;\psi'\Big(\frac{2-\tilde{m}}{2}\Big)\;-\;\psi'\Big(\frac{1-\tilde{m}}{2}\Big)\\
&= \sum_{r=0}^{\infty}\frac{1}{(r+\frac{3}{4}+\frac{n}{4}+\frac{i\nu}{2})^2}\;-\;\sum_{r=0}^{\infty}\frac{1}{(r+\frac{1}{4}+\frac{n}{4}+\frac{i\nu}{2})^2}\\
&\quad+\;\sum_{r=0}^{\infty}\frac{1}{(r+\frac{3}{4}+\frac{n}{4}-\frac{i\nu}{2})^2}\;-\;\sum_{r=0}^{\infty}\frac{1}{(r+\frac{1}{4}+\frac{n}{4}-\frac{i\nu}{2})^2}
\end{aligned} \tag{7.17}$$

We next show that this expression is unchanged if we simultaneously send $m \to 1-m$ and $\tilde{m} \to 1-\tilde{m}$, i.e. $n \to -n,\ \nu \to -\nu$. At this point it is crucial that $n$ is an even integer. Writing $n = 2M$, we obtain

$$\begin{aligned}
16\pi\Lambda(-\nu,-n) \;=&\sum_{r=0}^{\infty}\frac{1}{(r+\frac{1}{4}+\frac{-M+1}{2}-\frac{i\nu}{2})^2}\;-\;\sum_{r=0}^{\infty}\frac{1}{(r+\frac{1}{4}+\frac{-M}{2}-\frac{i\nu}{2})^2}\\
&+\;\sum_{r=0}^{\infty}\frac{1}{(r+\frac{1}{4}+\frac{-M+1}{2}+\frac{i\nu}{2})^2}\;-\;\sum_{r=0}^{\infty}\frac{1}{(r+\frac{1}{4}+\frac{-M}{2}+\frac{i\nu}{2})^2}
\end{aligned} \tag{7.18}$$

and so

$$\begin{aligned}
16\pi(\Lambda(-\nu,-n)\;-\;\Lambda(\nu,n)) \;&=\;\sum_{s=-M}^{-1}\frac{1}{(s+\frac{1}{4}+\frac{M+1}{2}-\frac{i\nu}{2})^2}\;-\;\sum_{s=-M}^{-1}\frac{1}{(s+\frac{1}{4}+\frac{M}{2}-\frac{i\nu}{2})^2}\\
&\quad+\;\sum_{s=-M}^{-1}\frac{1}{(s+\frac{1}{4}+\frac{M+1}{2}+\frac{i\nu}{2})^2}\;-\;\sum_{s=-M}^{-1}\frac{1}{(s+\frac{1}{4}+\frac{M}{2}+\frac{i\nu}{2})^2}\\
&=\;\sum_{t=-M/2}^{M/2\;-1}\frac{1}{(t+\frac{3}{4}-\frac{i\nu}{2})^2}\;-\;\sum_{t=-M/2}^{M/2\;-1}\frac{1}{(-t-\frac{3}{4}-\frac{i\nu}{2})^2}\\
&\quad+\;\sum_{t=-M/2}^{M/2\;-1}\frac{1}{(t+\frac{3}{4}+\frac{i\nu}{2})^2}\;-\;\sum_{t=-M/2}^{M/2\;-1}\frac{1}{(-t-\frac{3}{4}+\frac{i\nu}{2})^2}\\
&=\;0
\end{aligned} \tag{7.19}$$

Because of this last symmetry, we can write

$$16\pi\Lambda(\nu,n) \;=\; -\;2\Big(\beta'(m) \;+\; \beta'(1-m) \;+\; \beta'(1-\tilde{m})\Big) \;+\; \beta'(\tilde{m})\Big) \tag{7.20}$$

The final result needed to write (7.16) is that

$$\begin{aligned}\psi'\Big(\frac{m}{2}\Big) \;+\; \psi'\Big(\frac{1-m}{2}\Big) \;&=\; \sum_{r=0}^{\infty}\frac{2r^2+r+1/4-m(1-m)/2}{\big[r^2+r/2+m(1-m)/2\big]^2}\\ &=\tilde{\mathcal{F}}_1[m(1-m)]\end{aligned} \tag{7.21}$$

and similarly

$$\psi'\Big(\frac{m+1}{2}\Big) \;+\; \psi'\Big(\frac{1-m+1}{2}\Big) \;=\; \tilde{\mathcal{F}}_2[m(1-m)]\;. \tag{7.22}$$

This then allows us to write (7.16) with

$$\mathcal{G}[m(1-m)] \;=\; \frac{1}{8\pi}\Big(\tilde{\mathcal{F}}_1[m(1-m)] \;-\; \tilde{\mathcal{F}}_2[m(1-m)]\Big)\;. \tag{7.23}$$

Finally we discuss the numerical values that we obtain from our results. The leading eigenvalue is at at $\nu = n = 0$, as it is for the $O(g^2)$ kernel. As we see from (7.3), the correction to $\alpha_0$ is given by $\mathcal{E}(0,0)/(16\pi^3)$. To evaluate this we use

$$\begin{aligned}\Lambda(0,0) \;&=\; -\;\frac{1}{2\pi}\beta'(1/2)\\ &=\; -\;\frac{1}{8\pi}\Big(\sum_{r=0}^{\infty}\frac{1}{(r+\;1/4)^2} \;-\; \sum_{r=0}^{\infty}\frac{1}{(r+\;3/4)^2}\Big)\\ &=\; -\;\frac{1}{8\pi}\Big(\;16\;+\;\frac{16}{25}\;+\;\frac{16}{81}\;+\;...\;-\;\frac{16}{9}\;-\;\frac{16}{49}\;+\;...\Big)\\ &\sim\; -\;\frac{1.81}{\pi}\end{aligned} \tag{7.24}$$

From $\mathcal{K}_2$ alone we obtain

$$\frac{9g^4}{16\pi^3}\Lambda(0,0) \;\sim\; -\,16.3\frac{{\alpha_s}^2}{\pi^2} \tag{7.25}$$

The complete $\hat{K}^{(4n)}$ gives

$$\begin{aligned}\mathcal{E}(0,0)/(16\pi^3) \;&\sim\; \frac{N^2g^4}{16\pi^4}\Big([2ln2]^2 \;-\; 1.81\Big)\\ &\sim\; \frac{9g^4}{16\pi^4}\times 0.11 \;\sim\; \frac{{\alpha_s}^2}{\pi^2}\end{aligned} \tag{7.26}$$

giving a very small positive effect.

At this point we note that while $\mathcal{K}_1$ and $\mathcal{K}_2$ can consistently be added to the leading-order kernel, this is not the case for $\mathcal{K}_0$. Although $\mathcal{K}_0$ is needed to regulate $\mathcal{K}_1 \ + \ \mathcal{K}_2$, it contains the $K_0^{(4)}$ diagrams which, as we emphasized in [3], can not be interpreted in terms of reggeization effects. Since reggeization is the only consistent interpretation of disconnected pieces, the $K_0^{(4)}$ diagrams can not be present in the full kernel. As we described in [4], to eliminate these diagrams while retaining scale-invariance it is necessary to consider

$$\tilde{K}_{2,2}^{(4)} \ = \ \hat{K}_{2,2}^{(4n)} \ - \ \left(\hat{K}_{2,2}^{(2)}\right)^2 \ , \tag{7.27}$$

This is a consistent scale-invariant $O(g^4)$ kernel which can be added to the $O(g^2)$ kernel. In this case, in writing (7.3), we replace $\mathcal{E}(\nu, n)$ by $\tilde{\mathcal{E}}(\nu, n)$ where

$$\tilde{\mathcal{E}}(\nu, n) \ = \ - \ \frac{3}{\pi}[\chi(\nu, n)]^2 \ - \ \Lambda(\nu, n) \ . \tag{7.28}$$

This gives, as a modification of $\alpha_0$,

$$\begin{aligned} \frac{\tilde{\mathcal{E}}(0,0)}{16\pi^3} \ &= \frac{N^2 g^4}{16\pi^4}\Big(-3[\chi(0,0)]^2 \ - \ \Lambda(0,0)\Big) \\ &\sim \frac{9g^4}{16\pi^4} \times (-5.76 - 1.81) \\ &\sim \ -68\frac{{\alpha_s}^2}{\pi^2} \end{aligned} \tag{7.29}$$

which is a substantial negative correction. We briefly discuss general questions related to the significance of these numbers in the next, concluding, Section. They clearly show that, at next-to-leading-order, the infra-red region can produce a strong reduction of the BFKL small-x behavior.

## 8. CONCLUSIONS

We have presented a variety of properties of the $O(g^4)$ kernel which appears as an infra-red effect in the next-to-leading order BFKL equation. We have emphasized the parallel between the mathematical properties of this new kernel and the leading-order BFKL kernel. We have not addressed its general significance. Indeed, in a recent

paper Lipatov[13] has argued that the kernel obtained by direct next-to-leading order calculations will be more complicated than our kernel and, in general, will not reduce to transverse momentum integrals.

In a companion paper [5] we show that the kernels we have studied unambigously arise when the $t$-channel unitarity equations are, in a weak-coupling approximation, systematically expanded in the angular momentum plane around $j = 1$, while keeping the leading particle singularities. Consequently the kernels we have studied must be obtainable as infra-red (in transverse momentum) approximations to the full next-to-leading log kernel calculated in momentum space[13]. We find that $K^{4n}$ enters directly as a next-to-leading order scale-invariant contribution. $(K^{(2)})^2$ also appears at next-to-leading-order but, simultaneously, internal transverse momentum logarithms appear which violate the scale-invariance. These are the logarithms found by Fadin and Lipatov[14] in the higher-order trajectory function. Therefore it is not clear that is sensible to maintain scale-invariance when introducing $(K^{(2)})^2$.

Since the $t$-channel unitarity equations are infra-red constraints, the use of transverse-momentum integrals may only be valid below some transverse momentum cut-off. For applications to small-x physics at relatively large transverse momentum, this cut-off could be crucial for a reliable estimate of the relative magnitude of our contributions in the full physical kernel. Because of this, the numerical results we obtain tell us only the size of effects that are obtained by naively extending the infra-red behaviour of the theory to arbitrarily large transverse momentum. In this context we should remark that it is not yet clear that the program of [13] leads to a next-to-leading order kernel that can be consistently evaluated at large transverse momentum - with the running coupling properly involved.

Ultimately it is the Regge limit of QCD which is of most theoretical interest. The Regge region is truly the infra-red region in transverse momentum and this is what $t$-channel unitarity is best suited to studying. We argue in our companion paper that the expansion techniques we develop, when properly limited to the infra-red region, are likely to be very powerful in providing very high-order information on the Regge limit. Indeed, we believe the scale-invariant kernels we derive may play a fundamental role in understanding the true nature of the soft Pomeron as a full solution of QCD at asymptotic energies.

It is from this last perspective that it seems most important to study to what extent fundamental properties of the leading-order kernel, such as holomorphic factorization and conformal symmetry, are preserved in higher-order scale-invariant kernels.

That the eigenvalue spectrum of the $O(g^4)$ kernel does indeed have such properties, seems to us both interesting and intriguing.

**Acknowledgements**

We thank J. Bartels, V. Fadin, R. Kirschner and L. Lipatov for informative discussions and comments. C.C. is grateful to B. Andersson, Yu. L. Dokshitzer and to G. Marchesini for very formative lectures and discussions at Lund Univ. and at St. Petersburg's winter school.

## Appendix A. Kinematics

We review here some kinematic features which are special to two dimensions and which complicate our analysis.

In two dimensions there is only one independent two-particle invariant in elastic scattering. That is both $t$ and $u$ can be choosen to be functions of $s$ which, as usual we interpret as the total energy. In fact, consider a 2-to-2 particle scattering $k_1 + k_2 \;\rightarrow\; k_3 + k_4$. If we define

$$z_i \;=\; k_i^2 \quad i \;=\; 1,..,4,$$

then in the center of mass we have

$$\begin{aligned}
k_1 &= \frac{1}{2\sqrt{s}}\left(s - {k_2}^2 + {k_1}^2, \lambda^{1/2}(s, k_1^2, k_2^2)\right)\\
k_2 &= \frac{1}{2\sqrt{s}}\left(s + {k_2}^2 - {k_1}^2, -\lambda^{1/2}(s, k_1^2, k_2^2)\right)\\
k_3 &= \frac{1}{2\sqrt{s}}\left(s + k_3^2 - k_4^2, \lambda^{1/2}(s, k_3^2, k_4^2)\right)\\
k_4 &= \frac{1}{2\sqrt{s}}\left(s - k_3^2 + k_4^2, -\lambda^{1/2}(s, k_3^2, k_4^2)\right).
\end{aligned} \tag{A.1}$$

One still defines the Mandelstam invariants as in D=4: $s$, $t = (k_3 - k_1)^2$ and $u = (k_1 - k_4)^2$, and verifies that they satisfy the usual Mandelstam relation

$$s + t + u = (k_1^2 + k_2^2 + k_3^2 + k_4^2)\ . \tag{A.2}$$

From (A.1), however, it is easy to derive the relations

$$t = \frac{k_1^2 + k_2^2 + k_3^2 + k_4^2 - s}{2} - \frac{(-k_2^2 + k_1^2)(-k_4^2 + k_3^2) - \lambda^{1/2}(s, k_1^2, k_2^2)\lambda^{1/2}(s, k_3^2, k_4^2)}{2s}$$
$$u = \frac{k_1^2 + k_2^2 + k_3^2 + k_4^2 - s}{2} - \frac{(-k_2^2 + k_1^2)(k_4^2 - k_3^2) + \lambda^{1/2}(s, k_1^2, k_2^2)\lambda^{1/2}(s, k_3^2, k_4^2)}{2s}. \tag{A.3}$$

## Appendix B. Evaluation of the coefficients $A_{ij}$

In this Appendix we illustrate in some more detail the evaluation of the coefficients of the logarithms of the box diagram. As we emphasized in the text, it is crucial to use explicit expressions for the dual vectors $k^d{}_i$ in terms of the original external momenta $k_i$ in order to obtain a simple result for the $A_{ij}$'s. We first evaluate the $A_{ij}^{\pm}$ with a mass cut-off included.

Noting that from (4.12)

$$A_{12}^{\pm} = \frac{1}{((q_{12}^{\pm} - p_3)^2 + m^2)((q_{12}^{\pm} - p_4)^2 + m^2)} \tag{B.1}$$

we use the definition of $q_{12}^{\pm}$ in (4.6) to obtain

$$\begin{aligned}
&((q_{12}^{\pm} - p_3)^2 + m^2)((q_{12}^{\pm} - p_4)^2 + m^2) \\
&= \frac{1}{n_{12} z_1^2} \Big( z_1 z_2 + z_1 k_1 \cdot k_2 \pm n_{12} \lambda^{1/2}(-z_1, m^2, m^2) \Big) \\
&\quad \times (z_1(z_2 + z_3 - 2k_2 \cdot k_3 + k_1 \cdot k_2 - k_1 \cdot k_3) n_{12} \\
&\pm ((k_1 \cdot k_2)^2 - z_1 z_2 - k_1 \cdot k_3 k_1 \cdot k_2 + z_1 k_2 \cdot k_3) \lambda^{1/2}(z_1, m^2, m^2) \Big)
\end{aligned} \tag{B.2}$$

where

$$z_i = k_i^2, \quad n_{ij} = \sqrt{(k_i \cdot k_j)^2 - z_i z_j}. \tag{B.3}$$

Similarly

$$A_{13}^{\pm} = \frac{1}{((q_{13}^{\pm} - p_2)^2 + m^2)(q_{13}^{\pm} - p_4)^2 + m^2)} \tag{B.4}$$

with

$$((q_{13}^{\pm} - p_2)^2 + m^2)(q_{13}^{\pm} - p_4)^2 + m^2)$$

$$= -\frac{k_1 \cdot k_2}{s} \left(s \;\; n_{12}(z_3 - k_1 \cdot k_3 - k_2 \cdot k_3)\right.$$
$$\left. \pm \lambda^{1/2}(s, m^2, m^2)(k_1 \cdot k_3 k_1 \cdot k_2 + k_2 \cdot k_3 k_1 \cdot k_2 - z_1 k_2 \cdot k_3 - z_2 k_1 \cdot k_3)\right)$$

$$A_{14}^{\pm} = \frac{1}{((q_{14}^{\pm} - p_2)^2 + m^2)(q_{14}^{\pm} - p_3)^2 + m^2)} \tag{B.5}$$

with

$$\begin{aligned}
&((q_{14}^{\pm} - p_2)^2 + m^2)((q_{14}^{\pm} - p_3)^2 + m^2) \\
&= \frac{1}{n_{34} k_4^2} \left(z_4(z_3 + z_2 - 2k_2 \cdot k_3 + k_3 \cdot k_4 - k_2 \cdot k_4) n_{34}\right. \\
&\quad \left. \pm (k_3 \cdot k_4 k_2 \cdot k_4 - k_3 \cdot k_4 k_3 \cdot k_4 - z_4(k_2 \cdot k_3 - z_2)) \lambda^{1/2}(k_4^2, m^2, m^2)\right) \\
&\quad \times \left(z_3 z_4 + z_4 k_3 \cdot k_4 \pm n_{34} \lambda^{1/2}(-k_4^2, m^2, m^2)\right)
\end{aligned} \tag{B.6}$$

$$A_{23}^{\pm} = \frac{1}{((q_{23}^{\pm} - p_4)^2 + m^2)(q_{23}^{\pm} - p_1)^2 + m^2)} \tag{B.7}$$

with

$$\begin{aligned}
&((q_{23}^{\pm} - p_4)^2 + m^2)((q_{23}^{\pm} - p_1)^2 + m^2) \\
&= \frac{1}{n_{12} z_2^2} \left(z_1 z_2 + z_2 k_1 \cdot k_2 \mp n_{12} \lambda^{1/2}(z_2, m^2, m^2)\right) \\
&\quad \times \left((z_2 z_3 - z_2 k_2 \cdot k_3) n_{12} \mp (k_2 \cdot k_3 k_1 \cdot k_2 - z_2 k_1 \cdot k_3) \lambda^{1/2}(z_2, m^2, m^2)\right)
\end{aligned} \tag{B.8}$$

$$A_{24}^{\pm} = \frac{1}{((q_{24}^{\pm} - p_1)^2 + m^2)(q_{24}^{\pm} - p_3)^2 + m^2)} \tag{B.9}$$

with

$$\begin{aligned}
&((q_{24}^{\pm} - p_1)^2 + m^2)((q_{24}^{\pm} - p_3)^2 + m^2) \\
&= \frac{1}{(k_1 - k_3)^2 n_{12}^2 n_{34}} \left(n_{12} n_{34}(z_1 - k_1 \cdot k_3 + k_1 \cdot k_2)(k_2 - k_3)^2 \pm H_{24,1}\right) \\
&\quad \left(k_2 \cdot k_3 (k_2 - k_3)^2 n_{12} \pm H_{24,3}\right)
\end{aligned} \tag{B.10}$$

where

$$H_{24,1} = \Big((k_1\cdot k_2)^2 - z_1 z_2\Big)\, n_{34} - (k_1\cdot k_3 k_3\cdot k_4 - z_3 k_1\cdot k_4)\,\lambda^{1/2}((k_2-k_3)^2, m^2, m^2)$$
$$H_{24,3} = (k_2\cdot k_3 k_1\cdot k_2 - z_2 k_1\cdot k_3)\,\lambda^{1/2}((k_2-k_3)^2, m^2, m^2) \tag{B.11}$$

Finally

$$A_{34}^{\pm} = \frac{1}{((q_{34}^{\pm}-p_1)^2+m^2)(q_{34}^{\pm}-p_2)^2+m^2)} \tag{B.12}$$

with

$$\begin{aligned}&((q_{34}^{\pm}-p_1)^2+m^2)((q_{34}^{\pm}-p_2)^2+m^2)\\ &= \frac{1}{z_3^2 n_{34}}\Big(z_1+z_2+2k_1\cdot k_2 - k_1\cdot k_3 - k_2\cdot k_3 \mp n_{34}\lambda^{1/2}(k_3^2, m^2, m^2)\Big)\\ &\times \quad \Big((z_2 z_3 - z_3 k_2\cdot k_3)n_{34} \mp H_{34,2}\lambda^{1/2}(k_3^2, m^2, m^2)\Big)\end{aligned} \tag{B.13}$$

where

$$H_{34,2} = k_2\cdot k_3 k_3\cdot k_4 - z_2 k_2\cdot k_4. \tag{B.14}$$

Notice that all the coefficients $A_{ij}$ can be re-expressed in terms of the invariant $s = (k_1+k_2)^2$ quite straightforwardly.

It is because each dual vector contains non-integer powers of the $\Lambda$-function that it is useful to combine the single contributions $A_{ij}^{\pm}$ with a single common denominator, to obtain a simple polynomial result. Combining this with the massless limit leads to the $A_{ij} \equiv a_{ij}/b_{ij}$ utilised in the text. The $a_{ij}$ and $b_{ij}$ that we did not give explicitly in Section 4 are

$$\begin{aligned}b_{34} = &\Big[-\Big(-k_2\cdot k_4\, {k_3}^2 + k_2\cdot k_3\, k_3\cdot k_4\Big)^2 + ({k_2}^2 - k_2\cdot k_3)^2\,(k_3\cdot {k_4}^2 - {k_3}^2\,{k_4}^2)\Big]\\ &\times\Big[-\Big(-(k_1\cdot k_4 + k_2\cdot k_4)\,{k_3}^2 + (k_1\cdot k_3 + k_2\cdot k_3)\,k_3\cdot k_4\Big)^2\\ &\quad +({k_1}^2 + 2\,k_1\cdot k_2 - k_1\cdot k_3 + {k_2}^2 - k_2\cdot k_3\ )^2\,(k_3\cdot {k_4}^2 - {k_3}^2\,{k_4}^2)\Big]\end{aligned}$$

$$\begin{aligned}a_{14} = &\Big[k_3\cdot {k_4}^2 - {k_3}^2\,{k_4}^2\Big]\\ &\times\Big[k_3\cdot k_4\,(-k_2\cdot k_4 + k_3\cdot k_4)\end{aligned}$$

$$+({k_3}^2 + k_3 \cdot k_4)\,({k_2}^2 - 2\,k_2 \cdot k_3 - k_2 \cdot k_4 + {k_3}^2 + k_3 \cdot k_4) - ({k_3}^2 - k_3 \cdot k_4)\,{k_4}^2\Big] \tag{B.15}$$

$$\begin{aligned} b_{14} = &\Big[-k_3 \cdot {k_4}^2 + ({k_3}^2 + k_3 \cdot k_4)^2 + {k_3}^2\,{k_4}^2\Big] \\ &\times\Big[({k_2}^2 - 2\,k_2 \cdot k_3 - k_2 \cdot k_4 + {k_3}^2 + k_3 \cdot k_4)^2\,(k_3 \cdot {k_4}^2 - {k_3}^2\,{k_4}^2) \\ &-[k_3 \cdot k_4\,(-k_2 \cdot k_4 + k_3 \cdot k_4) - ({k_3}^2 - k_3 \cdot k_4)\,{k_4}^2]^2\Big] \end{aligned} \tag{B.16}$$

$$\begin{aligned} a_{13} = &\Big[k_1 \cdot {k_2}^2 - {k_1}^2\,{k_2}^2\Big] \\ &\times\Big[k_1 \cdot k_2\,k_1 \cdot k_3 + k_1 \cdot k_3\,{k_2}^2 - {k_1}^2\,k_2 \cdot k_3 - k_1 \cdot k_2\,k_2 \cdot k_3 + k_1 \cdot k_2\,k_3 \cdot k_4\Big] \end{aligned} \tag{B.17}$$

$$\begin{aligned} b_{13} = &{k_1}^2{k_2}^2\,\Big[-(k_1 \cdot k_2\,k_1 \cdot k_3 + k_1 \cdot k_3\,{k_2}^2 - {k_1}^2\,k_2 \cdot k_3 - k_1 \cdot k_2\,k_2 \cdot k_3)^2 \\ &+({k_1} \cdot {k_2}^2 - {k_1}^2\,{k_2}^2)\,k_3 \cdot {k_4}^2\Big] \end{aligned} \tag{B.18}$$

$$\begin{aligned} a_{24} = &\Big[k_1 \cdot k_3\,{k_2}^2 - k_1 \cdot k_2\,k_2 \cdot k_3 + ({k_1}^2 + k_1 \cdot k_2 \\ &-k_1 \cdot k_3)\,k_2 \cdot k_3 - k_1 \cdot k_3\,k_2 \cdot k_3 + k_1 \cdot k_2\,{k_3}^2\Big]\Big[k_2 \cdot {k_3}^2 - {k_2}^2\,{k_3}^2\Big] \end{aligned} \tag{B.19}$$

$$\begin{aligned} b_{24} = &{k_2}^2{k_3}^2\Big[-(k_1 \cdot k_3\,{k_2}^2 - k_1 \cdot k_2\,k_2 \cdot k_3 - k_1 \cdot k_3\,k_2 \cdot k_3 + k_1 \cdot k_2\,{k_3}^2)^2 \\ &+({k_1}^2 + k_1 \cdot k_2 - k_1 \cdot k_3)^2\,(k_2 \cdot {k_3}^2 - {k_2}^2\,{k_3}^2)\Big] \end{aligned} \tag{B.20}$$

## Appendix C. Dual Vectors

The definitions of the dual vectors $k_i^d$ eq. (4.8) in terms of the external momenta $k_i$ are not unique. For instance we could have defined

$$
\begin{aligned}
{k^d}_1 &= \frac{\epsilon(n_{13})}{\sqrt{(k_1\cdot k_3)^2 - k_1^2 k_3^2}}\left(k_1 k_1\cdot k_3 - k_3 k_1^2\right) \\
{k^d}_2 &= -\frac{\epsilon(n_{23})}{\sqrt{(k_2\cdot k_3)^2 - k_2^2 k_3^2}}\left(k_2 k_2\cdot k_3 - k_3 k_2^2\right),
\end{aligned}
\tag{C.1}
$$

and similar others. It is also easily shown that

$$
\begin{aligned}
\lambda(t, k_1^2, k_3^2) &= \epsilon(n_{13})((k_1\cdot k_3)^2 - k_1^2 k_3^2) \\
\lambda(u, k_1^2, k_4^2) &= \epsilon(n_{14})((k_1\cdot k_4)^2 - k_1^2 k_4^2).
\end{aligned}
\tag{C.2}
$$

Nontrivial relations between $\Lambda$-functions can also be derived e.g.

$$
\lambda^{1/2}(s, k_1^2, k_2^2)\lambda^{1/2}(t, k_1^2, k_3^2) \;=\; 4(k_1\cdot k_2 k_2\cdot k_3 - k_2^2 k_1\cdot k_3) \tag{C.3}
$$

and

$$
\frac{\lambda^{1/2}(t, k_2^2, k_3^2)}{\lambda(s, k_1^2, k_2^2)} \;=\; \frac{\epsilon(n_{23})(k_1\cdot k_3 k_2\cdot k_3 - k_3^2 k_1\cdot k_2)}{\epsilon(n_{12})(k_1\cdot k_3 k_1\cdot k_2 - k_1^2 k_2\cdot k_3)} \tag{C.4}
$$

(valid for positive values of the left-hand sides) in the Minkowsky region. In the euclidean region, exploiting the $\lambda$-function as an area (see Fig. C.1) gives

$$
\lambda^{1/2}(s, k_1^2, k_2^2) + \lambda^{1/2}(s, k_3^2, k_4^2) = \lambda^{1/2}(t, k_1^2, k_3^2) + \lambda^{1/2}(t, k_2^2, k_4^2). \tag{C.5}
$$

The existence of these relations is what makes simplification of the coefficients $A_{ij}$ non-trivial.

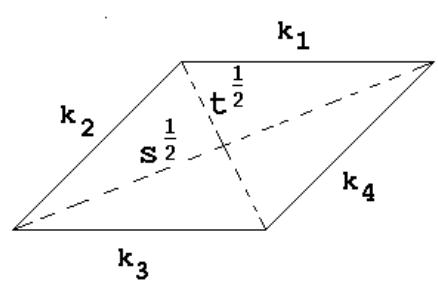

Fig. C.1 Euclidean triangles

## Appendix D. Analyticity Properties.

In this Appendix we discuss some aspects of the analyticity properties and dispersion theory of one-loop n-point functions at $D = 2$. Note first that in the special case in which any of the external momenta becomes exceptional, the Kallen-Toll method is not applicable. Nevertheless it is still possible to evaluate directly the box diagram integral, for example, from its dispersive part, i.e. we write

$$I(k_1, k_2, k_3, k_4) = \frac{1}{4\pi} \int_{4m^2}^{\infty} dz \frac{\Delta(z)}{(z-s)} \tag{D.1}$$

where

$$\Delta(z) = \frac{\sqrt{z-4m^2}\lambda[z, k_1^2, k_2^2]^{1/2}\lambda[s, k_3^2, k_4^2]^{1/2}}{(4m^2\lambda[z, k_1^2, k_2^2] + 4zk_1^2k_2^2)(4m^2\lambda[z, k_3^2, k_4^2] + 4zk_3^2k_4^2)} \tag{D.2}$$

is the $s-$channel cut of the box diagram

$$\Delta(s) = \int d^4\, q \frac{\delta_+(q^2-m^2)\delta_+((k_1+k_2-q)^2-m^2)}{[(k_1-q)^2-m^2][k_2-q)^2-m^2]} \tag{D.3}$$

The dispersion integral is not straightforward, in the general case, and involves also elliptic functions. The logarithmic structure may appear only after non-trivial manipulations. However, in the case of exceptional external momenta it provides a simple alternative to the method of residui. We remark that all the one-loop functions can be re-obtained by dispersive methods quite elementarily. This is particularly simple when, as in our case, the internal masses are equal and so there is no contribution from anomalous thresholds.

We also observe that the 2-point function

$$I(q^2) \;=\; = \; 16\pi^3 J_1(q^2, m^2) \;=\; \int \frac{dp}{(p^2+m^2)((q-p)^2+m^2} \tag{D.4}$$

can be written down in various forms. These forms may differ by the choice of phase conventions for the logarithms involved. For instance one easily obtains

$$I(q) = \frac{\theta}{m^2 sinh\ \theta} \qquad\qquad cosh\ \theta = \frac{q^2+2m^2}{2m^2} \tag{D.5}$$

which in its logarithmic form becomes

$$I(q) = \frac{2}{\sqrt{q^2(q^2+4m^2)}} Log\left(\frac{q^2+2m^2 \pm \sqrt{q^2+4m^2}}{2m^2}\right). \tag{D.6}$$

If we choose either the " + " or " - " determination of the logarithm in (D.6), we encounter a branch cut at $q^2 = -4m^2$ and *no* threshold singularity (at $q = 0$), as expected. Combinining both determinations, instead, we obtain the Kallen-Toll result for $I(q)$ quoted in Section 4 which is free of any singularity in the finite plane. In our case the distinction is not essential, since we are only interested in real parts obtained in the massless limit.

## Appendix E. Identities.

In Dimensional Regularization we get

$$\frac{1}{[k^2]^\alpha} = \frac{\Gamma[D/2-\alpha]}{\Gamma[\alpha]\pi^{D/2}} \int \frac{d^D x e^{2ik\cdot x}}{[x^2]^{D/2-\alpha}}. \tag{E.1}$$

Using this relation we find a simple expression for the integral

$$\begin{aligned} I[R,S] &= \int \frac{d^D k}{[(k-q)^2]^R [k^2]^S} \\ &= \frac{\Gamma[D/2-R]\Gamma[D/2-S]}{(2\pi)^D \Gamma[R]\Gamma[S]} \int \frac{d^D x e^{2iq\cdot x}}{[x^2]^{D/2-\sigma}} \\ &, \end{aligned} \tag{E.2}$$

where $\sigma = R + S - D/2$. A simple manipulation of this expression gives

$$I[R,S] = \frac{1}{[q^2]^{R+S-D/2}} \frac{\Gamma[D/2-R]\Gamma[D/2-S]\Gamma[R+S-D/2]}{\pi^{D/2} 2^D \Gamma[R]\Gamma[S]\Gamma[D-R-S]} \tag{E.3}$$

$J_1(k^2)$ is immediately evaluated as in the text. For $J_2(k^2)$ we obtain

$$\begin{aligned} J_2(k^2) &\equiv \int d^D p \frac{J_1(p)}{(k-p)^2} \\ &= \frac{1}{[k^2]^{3-D}} \frac{\eta\ \pi^{D/2}\Gamma[D/2-1]\Gamma[D-2]\Gamma[3-D]}{\Gamma[2-D/2]\Gamma[3D/2-3]}. \end{aligned} \tag{E.4}$$

Writing $D = 2 + \epsilon$ we obtain

$$k^2 J_2(k^2) = 6\gamma^2\pi^2 - \frac{\pi^4}{2} + \frac{12\pi^2}{\epsilon^2} + \frac{12\gamma\pi^2}{\epsilon} + 12\gamma\pi^2\log(\pi) + \frac{12\pi^2\log(\pi)}{\epsilon} + 6\pi^2[\log(\pi)]^2$$
$$+12\gamma\pi^2\log(k^2) + \frac{12\pi^2\log(k^2)}{\epsilon} + 12\pi^2\log(\pi)\log(k^2) + 6\pi^2[\log(k^2]^2. \tag{E.5}$$

Similarly we obtain

$$\left(k^2 J_1(k)\right)^2 = 8\gamma^2\pi^2 - \frac{2\pi^4}{3} + \frac{16\pi^2}{\epsilon^2} + \frac{16\gamma\pi^2}{\epsilon} + 16\gamma\pi^2\log(\pi) + \frac{16\pi^2\log(\pi)}{\epsilon} + 8\pi^2[\log(\pi)]^2$$
$$+16\gamma\pi^2\log(k^2) + \frac{16\pi^2\log(q^2)}{\epsilon} + 16\pi^2\log(\pi)\log(k^2) + 8\pi^2[\log(k^2)]^2\ , \tag{E.6}$$

We can also extract the leading double logarithmic contributions by introducing a mass cutoff. That is we write

$$J_2(k^2) \to J_2(k^2, m^2) = \int \frac{d^2q}{[(k-q)^2 + m^2]} \int \frac{d^2l}{[l^2 + m^2][(l-q)^2 + m^2]} \tag{E.7}$$

Perfoming the $l$ integral and one angular integral, and dropping the cutoff dependence whenever possible we get

$$J_2(k^2, m^2) = -\pi \int_0^\infty \frac{d\,q^2}{(k^2 + q^2)\sqrt{q^2(q^2 + 4m^2)}} Log[\chi(q^2)],$$
$$\chi(q^2) = \frac{1 - \sqrt{1 - 4m^2/q^2}}{1 + \sqrt{1 - 4m^2/q^2}}. \tag{E.8}$$

Defining the change of variable

$$x = \chi(q^2), \quad if \quad q^2 \neq 0$$
$$x = -1 \quad if \quad q^2 = 0 \tag{E.9}$$

some manipulations allow us to rewrite the integral in the form

$$J_2(k^2, m^2) = \pi \int_1^\infty d\ x\ \frac{Log[x]}{(x+x_0)(x+x_0')} \tag{E.10}$$

with

$$x_0 = \frac{1}{x_0'} = \frac{1+\sqrt{1+4m^2/q^2}}{1-\sqrt{1+4m^2/q^2}}. \tag{E.11}$$

The last integration in (E.10) can be easily performed by using

$$\int_0^z dx\ \frac{Log(x-a)}{x-b} = \left[\ Sp\Big[\frac{a-b}{x-b}\Big] + \frac{1}{2}Log[x-b]^2\ \right]_1^z \tag{E.12}$$

to obtain

$$J_2(k^2, m^2) = \frac{\pi}{2(x_0'-x_0)}\Big(Log^2[1+x_0'] - Log^2[1+x_0]\Big) \tag{E.13}$$

which clearly exhibits the $Log^2[m^2/k^2]$ contributions.

## Appendix F. Impact Parameter Space.

We note first that the contours in (6.11) separate the right and left poles of the $\Gamma$ functions. The contour can be closed in various possible ways, thus generating ascending and descending series, as usually happens for the Mellin transform. To derive the Gegenbauer expansion of the Y, at some special value of the powers of the propagators, we proceed as follows.

Following ref. [12] we start by defining

$$S_\lambda \equiv \frac{2\pi^{\lambda+1}}{\Gamma[\lambda+1]} \tag{F.1}$$

and introduce the expansion

$$\frac{1}{[(p-q)^2]^\lambda} = \frac{1}{{d_>}^{2\lambda}(p,q)} \sum_{n=0}^\infty {d_<}^n(p,q) C_n^\lambda(\hat{p}\cdot\hat{q}). \tag{F.2}$$

We have defined

$$\begin{aligned} d_<(p,q) &= min(\frac{p}{q}, \frac{q}{p}) \\ d_>(p,q) &= Max(p,q). \end{aligned} \tag{F.3}$$

The $D$ dimensional integration measures are then re-expressed as $d^D z = z^{2\lambda+1} S_\lambda d\hat{z}$ which isolates the $\hat{z}$ part of the integration. By using the orthogonality relation

$$\int d\hat{p} C^\lambda_{n_1}(\hat{k}\cdot\hat{p}) C^\lambda_{n_2}(\hat{p}\cdot q) = \delta_{n_1\, n_2} \frac{\lambda}{n_1+\lambda} C^\lambda_{n_1}(\hat{k}\cdot\hat{q}) \tag{F.4}$$

it is easy to derive the expression for $Y(\sigma_1, D/2-1, D/2-1|p,q)$ as a Gegenbauer series. The expression of $\mathcal{J}_n(x_+, x_-)$ is given by

$$\mathcal{J}_n(x_+, x_-) = \theta(x_+ - x_-) y(x_+, x_-) + \theta(x_- - x_+) y(x_-, x_+), \tag{F.5}$$

with

$$\begin{aligned} y(x_+, x_-) &= \frac{x_-^{2+n-2\sigma_1} x_+^{2-D-n}}{D+2n-2\sigma_1} \\ &+ \frac{x_+^{4-2\sigma_1-D-n} x_-^n}{2(1-\sigma_1)} - \frac{x_-^{2-2\sigma_1+n} x_+^{2-D-n}}{2(1-\sigma_1)} \\ &- \frac{x_-^n x_+^{4-n-2\sigma_1-D}}{4-2n-2\sigma_1-D} \end{aligned} \tag{F.6}$$

# References


[1] E. A. Kuraev, L. N. Lipatov, V. S. Fadin, *Sov. Phys. JETP* **45**, 199 (1977) ; Ya. Ya. Balitsky and L. N. Lipatov, *Sov. J. Nucl. Phys.* **28**, 822 (1978).

[2] A. R. White, *Phys. Lett.* **B334**, 87 (1994).

[3] C. Corianò and A. R. White ANL-HEP-CP-94-79, to be published in the Proceedings of the XXIV International Symposium on Multiparticle Dynamics, Vietri sul Mare, Italy (1994).

[4] C. Corianò and A. R. White ANL-HEP-PR-94-84, submitted to *Phys. Rev. Lett.*

[5] C. Corianò and A. R. White Argonne preprint, to appear.

[6] R. Kirschner, DESY Preprint (1994); L. N. Lipatov, *Phys. Lett.* **B251**, 284 (1990).

[7] L. N. Lipatov, in *Perturbative QCD*, ed. A. .H. Mueller (World Scientific, 1989).

[8] C. Destri and H.J. de Vega, *Nucl. Phys.* **B358**(1991), 251.

[9] G. Källen and J. Toll, *J. Math. Phys.* **6**(1965) 299.

[10] B. Berg, *Nuovo Cimento* **41A** (1977)58.

[11] Davydichev A.I., *J. Math. Phys.* **A25**, 5587 (1992); Boos E.E. and Davydichev A.I., *Teor. Mat. Fiz.* **89**, 56 (1991).

[12] Chetyrkin K.G., Kataev A.L. and Tkachov F.Y., *Nucl. Phys* **B45**, 345 (1980).

[13] L. N. Lipatov, DESY Preprint, DESY 95-029.

[14] V. S. Fadin, presentation at the Gran Sasso QCD Summer Institute (1994); V. S. Fadin and L. N. Lipatov, *Nucl. Phys.* **B406**, 259 (1993).